



Virginia Commonwealth University  
**VCU Scholars Compass**

---

Theses and Dissertations

Graduate School

---

2009

## DEVELOPMENT OF PPAR- $\gamma$ RECEPTOR AGONISTS AS THERAPEUTIC AGENTS FOR DIABETES

Ashwini Goswami  
*Virginia Commonwealth University*

Follow this and additional works at: <https://scholarscompass.vcu.edu/etd>

 Part of the [Chemicals and Drugs Commons](#)

© The Author

---

Downloaded from

<https://scholarscompass.vcu.edu/etd/1881>

This Thesis is brought to you for free and open access by the Graduate School at VCU Scholars Compass. It has been accepted for inclusion in Theses and Dissertations by an authorized administrator of VCU Scholars Compass. For more information, please contact [libcompass@vcu.edu](mailto:libcompass@vcu.edu).

© Ashwini Goswami 2009

All Rights Reserved

# **DEVELOPMENT OF PPAR- $\gamma$ RECEPTOR AGONISTS AS THERAPEUTIC AGENTS FOR DIABETES**

A thesis submitted in partial fulfillment of the requirements for the degree of M.S. at  
Virginia Commonwealth University.

By

ASHWINI GOSWAMI

Director: Dr. Martin K. Safo, Ph.D.  
Assistant Professor, Department of Medicinal Chemistry

Virginia Commonwealth University  
Richmond, Virginia  
May, 2009

## Acknowledgement

I would like to take this opportunity to thank my advisor, Dr. Martin K. Safo, for his assistance and guidance over the course of my research experience and also for the financial support, here at VCU. His support and insight have been invaluable in the progression of my research. I have appreciated his words of encouragement and support over the last few years.

My heartfelt thanks go to Dr. Richmond Danso-Danquah, who helped me in synthesis part of this project. I would like to thank Dr. Mohini S. Ghatage, who helped me in protein expression and purification. I would also like to thank Dr. Faik Musayev, from whom I learned valuable crystallographic techniques during my stay here at VCU.

I would like to thank Dr. Donald J. Abraham, for the financial support provided to me. I would also like also to acknowledge my appreciation for Drs. Darrell Peterson and Dr. Glen Kellogg for serving as my graduate committee members and for their assistance with this process. I appreciate the gift of PPAR- $\gamma$  plasmid from Dr. Igor Polikarpov from Universidade de Sao Paulo, Brazil.

I am also grateful to the staff at the VCU Department of Medicinal Chemistry and School of Pharmacy for making the logistics of this process as smooth as possible.

I would also like to show immense appreciation to my family, my mom and dad, who have provided countless moments of inspiration and motivation to achieve my goals.

I would not be the person I am today without them. I also thank my wife for her patience and support during my graduate school.

## Table of Contents

	Page
Acknowledgements .....	ii
List of Tables .....	viii
List of Figures .....	ix
List of Abbreviations.....	xi
List of Schemes.....	xiii
Abstract.....	xiv
Chapter	
I. Introduction.....	1
1. Nuclear Receptor .....	1
2. Nuclear Receptor Subtype .....	3
3. Estrogen Receptor.....	8
4. Peroxisome Proliferator Activated Receptor .....	9
5. Transcriptional Regulation by PPAR- $\gamma$ .....	10
6. Functional and Medicinal Roles of PPARs .....	14
7. Structure of PPAR .....	15
8. Ligand Binding Domain .....	17
9. Rationale and Hypothesis .....	21
II. EXPERIMENTAL METHODS.....	25

1. Expression and Purification of PPAR- $\gamma$ LBD .....	25
2. Molecular Modeling to Design PPAR- $\gamma$ Receptor Modulators.....	27
A. Design.....	27
B. Docking.....	30
3. Synthesis of Potential PPAR- $\gamma$ Receptor Modulators .....	32
A. Chemical Synthesis.....	32
a. Intermediates.....	33
5-(4-Amino-benzylidene)-thiazolidine-2,4-dione or <b>4</b> .....	33
b. Synthesis of Type-I compounds.....	33
N-[4-(2,4-Dioxo-thiazolidin-5-ylidenemethyl)-phenyl]-	
3-phenyl-propionamide or compound <b>A</b> .....	34
N-[4-(2,4-Dioxo-thiazolidin-5-ylidenemethyl)-phenyl]-	
2-(pyridin-3-yloxy)-acetamide or compound <b>D</b> .....	34
a. Synthesis of Type-II compounds.....	35
5-(3-Trifluoromethyl-phenyl)-furan-2-carboxylic	
acid [4-(2,4-dioxo-thiazolidin-5-ylidenemethyl)	
-phenyl]-amide or compound <b>B</b> .....	35
3-p-Tolyl-isoxazole-5-carboxylic acid [4-(2,4	
-dioxo-thiazolidin-5-ylidenemethyl)-phenyl]-amide or	
compound <b>C</b> .....	35
5-p-Tolyl-furan-2-carboxylic acid [4-(2, 4	
-dioxo-thiazolidin-5-ylidenemethyl)-phenyl]-	

amide or compound <b>F</b> .....	36
4. Functional Studies to Determine the Binding Affinity	
of PPAR- $\gamma$ Receptor Modulators.....	36
A. Assay Mechanism.....	36
B. Assay Procedure.....	37
5. Structural studies of PPAR- $\gamma$ LBD in complex with	
PPAR- $\gamma$ receptor modulators.....	39
A. Crystallization of Complex.....	39
 III. RESULTS AND DISSCUSSION.....	 41
1. Expression and Purification of PPAR- $\gamma$ LBD .....	41
2. Molecular Modeling to Design PPAR- $\gamma$ Receptor Modulators.....	44
3. Synthesis of Potential PPAR- $\gamma$ Receptor Modulators .....	51
A. Intermediates.....	51
B. Synthesis of Type-I compounds.....	51
C. Synthesis of Type-II compounds .....	54
4. Functional Studies to Determine the Binding Affinity	
of PPAR- $\gamma$ Receptor Modulators.....	56
5. Structural studies of PPAR- $\gamma$ LBD in complex with	



PPAR- $\gamma$ receptor modulators .....	58
IV SUMMARY AND CONCLUSION.....	60
References .....	62
VITA .....	76

## List of Tables

	Page
Table 1: NRs associated with metabolic disease, and their synthetic ligands. ....	7
Table 2: Yield of PPAR- $\gamma$ LBD protein with two different expression vectors. ....	44
Table 3: The percentage inhibition and IC-50 values by using Fluorescent Polarization Assay. ....	57

## List of Figures

	Page
Figure 1: Schematic diagrams for a common domain structure of Nuclear Receptors .....	3
Figure 2: Schematic diagrams for NR dimerization and DNA binding sequences.....	3
Figure 3: Human Nuclear Hormone Receptor Superfamily .....	4
Figure 4: Transcriptional activity of PPARs.....	13
Figure 5: Crystal structure of the apo-PPAR- $\gamma$ . ....	22
Figure 6: Crystal structure of PPAR- $\gamma$ LBD in complex with Rosiglitazone .....	22
Figure 7: Rosiglitazone in crystal structure with PPAR- $\gamma$ LBD .....	28
Figure 8: Structural components of PPAR- $\gamma$ LBD agonists .....	29
Figure 9: Fluorescent based affinity binding assay.....	37
Figure 10: Protein crystallization: Hanging drop vapor diffusion method .....	39
Figure 11: 10% SDS-PAGE gel of PPAR- $\gamma$ LBD protein purified using GST tag .....	43
Figure 12: 10% SDS-PAGE gel of PPAR- $\gamma$ LBD purified protein using His tag .....	43
Figure 13: Rosiglitazone in crystal structure with PPAR- $\gamma$ LBD .....	46
Figure 14: Proposed binding mode of Compound <b>A</b> (type-I compound) docked manually in PPAR- $\gamma$ LBD .....	47
Figure 15: Proposed binding mode of compound <b>A</b> (type-I compound) in the PPAR- $\gamma$ LBD complex.....	48
Figure 16: Proposed binding mode of compound <b>B</b> (type-II compound) docked manually in PPAR- $\gamma$ LBD .....	49
Figure 17: Proposed binding mode of compound <b>B</b> (type-II compound)	

in the PPAR- $\gamma$ LBD complex.....	50
--	----

## **List of Abbreviations**

AF	Activating Function
AIB1	Amplified In Breast Cancer-1
AR	Androgen Receptor
ARA-70	Androgen Receptor-Associated Protein
CBP	CREB Binding Protein
CAR	Constitutive Androstane Receptor
CREB	cAMP-response element binding protein
DBD	DNA-Binding Domain
DEC	N-(3-dimethylaminopropyl)-N-ethylcarbodiimide
DMF	N,N-dimethylformide
DMSO	Dimethyl Sulfoxide
DTT	Dithiothreitol
ESR	Estrogen Steroid Receptor
ER $\alpha$	Estrogen Receptor $\alpha$
FAAR	Fatty Acid Activated Receptor
FXR	Farnesoid X Receptor
GR	Glucocorticoid Receptor
GRIP1	Glucocorticoid Receptor Interacting Protein 1
GSH	Glutathione
GST	Glutathione S Transferase
HAT	Histone Acetyl Transferase
HNF	Hepatocyte Nuclear Factor Receptor
HOBt	1-hydroxybenzotriazole hydrate
KDa	Kilo Dalton
LBD	Ligand-Binding Domain
Log P <sub>o/w</sub>	Partition Coefficient for 1-Octanol/Water
LXR	Liver X Receptor
MAPK	Mitogen-Activated Protein Kinase
MR	Mineralocorticoid
$\mu$ M	Micromolar
NCOR	Nuclear Receptor Corepressor
NiNTA	Ni-nitrilotriacetic acid
NR	Nuclear Receptor
NR1C	Nuclear Receptor Nomenclature Committee
NUC1	NUClease 1
p300	Protein Coactivator 300
pCAF	p300/CBP-Associated Factor
PDB	Protein Data Bank
PGC-1 $\alpha$	PPAR- $\gamma$ Coactivator-1 $\alpha$
PPAR	Peroxisome Proliferator Activated Receptor
PPRE	Peroxisome Proliferator Response Element

PR	Progesterone Receptor
<sup>1</sup> H-NMR	Proton Nuclear Magnetic Resonance
PXR	Pregnane X Receptor
RAR	Retinoic Acid Receptor
RE	Response Elements
RIP-140	Receptor Interacting Protein-140
ROR	Cholesterol and Retinoic acid Receptor
RXR	Retinoid X Receptor
SF-1/ LRH-1	Steroidogenic Factor-1/ <i>Liver Receptor</i> Homologue-
<i>I</i>	
SRC-1	Steroid Receptor Coactivator-1
SMRT	Silencing Mediator for Retinoid and Thyroid
Receptors	
TF	Transcription Factors
THF	Tetrahydrofuran
TLC	Thin Layer Chromatography
TR	Thyroid Hormone Receptor
TZDs	Thiazolidinediones
VDR	Vitamin D Receptor
ZF	Zinc Fingers

## List of Schemes

	Page
Scheme 1: Synthesis of Intermediate <b>4</b> .....	52
Scheme 2: Synthesis of Type-I compounds .....	53
Scheme 3: Synthesis of Type-II compounds.....	55

## Abstract

# DEVELOPMENT OF PPAR- $\gamma$ RECEPTOR AGONISTS AS THERAPEUTIC AGENTS FOR DIABETES

By Ashwini Goswami, MS

A thesis submitted in partial fulfillment of the requirements for the degree of M.S. at  
Virginia Commonwealth University.

Virginia Commonwealth University, 2009

Major Director: Dr. Martin K. Safo, Ph.D.  
Assistant Professor, Department of Medicinal Chemistry

The peroxisome proliferator-activated receptors (PPARs) are the transcriptional regulators of glucose, lipids and cholesterol metabolisms. It has been established that PPAR- $\gamma$  is the receptor for thiazolidinediones (TZDs) class of type II anti-diabetic drugs. These compounds act as agonists of PPAR- $\gamma$ . They may delay the development of type II diabetes in individuals at high risk of developing the condition, and have been shown to have potentially beneficial effects on cardiovascular risk factors. PPAR- $\gamma$  receptor activation by TZDs improves insulin sensitivity by promoting fatty acid uptake into adipose tissue, increasing production of adiponectin (responsible for glucose regulation and fatty acid metabolism) and reducing levels of inflammatory mediators such as tumor necrosis factor- $\alpha$  (TNF- $\alpha$ ), plasminogen activator inhibitor-1 (PAI-1) and interleukin-6 (IL-6). Our goal is to take advantage of the mode of binding of known PPAR- $\gamma$  agonists, such as Rosiglitazone to PPAR- $\gamma$  to rationally design novel agonists of



PPAR- $\gamma$ . Our long-term objective is to generate new and potent PPAR- $\gamma$  agonists that could be used to treat diabetes. To achieve our goal the study was divided into five specific aims, including: **Aim 1.** Expression and purification of PPAR- $\gamma$  ligand binding domain (LBD). **Aim 2.** Molecular modeling to design PPAR- $\gamma$  receptor modulators. **Aim 3.** Synthesis of potential PPAR- $\gamma$  receptor modulators. **Aim 4.** Functional studies to determine the binding affinity of PPAR- $\gamma$  receptor modulators. **Aim 5.** Structural studies of PPAR- $\gamma$  LBD in complex with PPAR- $\gamma$  receptor modulators.

We expressed the His-tagged PPAR- $\gamma$  LBD protein in Rosetta DE3 cells, and used a one step affinity chromatography (Ni-NTA column) to obtain a significant yield of pure protein. Using the structural features and the known binding mode of Rosiglitazone to PPAR- $\gamma$  LBD as a starting point, two classes of compounds (type-I and type-II compounds) were designed as potential PPAR- $\gamma$  agonists. These novel compounds were rationalized to improve on the binding modes of Rosiglitazone via additional hydrogen-bonding and/or hydrophobic interactions to the protein. Five type-I and II compounds were synthesized and tested against PPAR- $\gamma$  receptor for binding affinity, using fluorescent polarization assay. The IC-50 value of the most potent compound (compound **B**) was found to be  $\sim 7$ -fold lower than Rosiglitazone, significantly lower than the expected value. It seems that unlike Rosiglitazone which has free rotatable thiazolidinedione ring that can make optimal interactions with His323 and His449 (two critical residues that are important for binding affinity), the thiazolidinedione ring in our compounds are fixed in one position that may not lead to optimal contact with the protein. We are currently synthesizing analogs of our compounds with rotatable thiazolidinedione ring for further studies. X-ray

crystallographic study has been initiated to determine the binding modes of our compounds with PPAR- $\gamma$  LBD which would allow for structural modifications for improving existing interactions and/or formation of new favorable interactions that could lead to higher affinity and potency. We have also initiated testing of these compounds to determine their PPAR- $\gamma$  agonistic effects.

## **{CHAPTER I Introduction}**

### **1. Nuclear Receptor**

Nuclear receptors (NR) are a class of proteins found within the interior of cells that regulate the expression of specific genes thereby controlling the development, homeostasis, and metabolism of the organism. These receptors are soluble proteins that can bind to specific DNA regulatory elements (response elements or REs) and act as cell type and promoter-specific regulators of transcription.<sup>1, 2</sup> In contrast to other transcription factors, the activity of nuclear receptors can be modulated by binding to the corresponding ligands, which are small lipophilic molecules that easily penetrate biological membranes. However, ligands for some of these nuclear receptors have not yet been identified. Nuclear receptors have been implicated in many physiological processes, such as cancer, diabetes, rheumatoid arthritis, asthma or hormone resistance syndromes.<sup>3</sup> As discussed in more detail below, nuclear receptors may be classified either according to mechanism or homology.<sup>4</sup>

In general, nuclear receptors act as homo- and heterodimers by binding to REs consisting of two copies of PuGGTCA core sequence. Many promoters whose transcription was shown to be nuclear receptor-dependent have been reported to contain nuclear receptor REs. There are also a great number of promoter and other gene regulatory

elements lacking REs but regulated by nuclear receptors through DNA-independent protein-mediated transcriptional control.<sup>5</sup> By virtue of this ligand-dependent activity, the nuclear hormone receptors serve as an interface between cellular or the whole body environment and our genome. The elucidation of the full length sequence of the first two founding members of the family, the human glucocorticoid receptor (GR) and estrogen receptor  $\alpha$  (ER $\alpha$ ) (cloned in 1985 and 1986, respectively) revealed a common domain structure as well as homology to the viral oncogene “v-erbA”, suggesting the existence of a receptor protein family.<sup>6</sup> Also in 1986, the cellular homologue of v-erb was discovered to be a receptor for thyroid hormone, indicating that ligands for the NRs are not limited to steroid hormones. Following, receptors for mineralocorticoid, progesterone, androgen and fat-soluble vitamins A and D were cloned, revealing extensive sequence similarity among these lipophilic hormone receptors.<sup>7</sup> Availability of genomic sequence information reveals that humans encode 48 NR family members and mice encode 49 NR family members.

During the last two decades, remarkable progress has been made toward the understanding of nuclear receptors in animal physiology, due to technological advancement in molecular genetics, genome wide target gene identification, single nucleotide polymorphism identification, and high throughput ligand identification. The notion that NRs integrate complex metabolic homeostasis is supported by systematic analyses of tissue-, time-, and stimuli-dependent NR gene expression.<sup>8</sup>

The NRs are defined by common structural motifs as depicted in Figure 1A. A highly variable NH<sub>3</sub>-terminal region contains a ligand-independent activation domain called AF-1. The central DNA-binding domain (DBD), consisting of two highly conserved zinc-

finger motifs unique to NRs, targets the receptor to specific DNA REs. Binding specificity by various receptors is largely achieved by the spacing (the 3-4-5 rule) and the orientation of two half-sites (direct-, inverted- or everted-repeat) (Figure 2). The hinge region confers structural flexibility in the receptor dimers allowing a single receptor dimer to interact with multiple RE sequences. The C-terminal ligand-binding domain (LBD) is functionally very unique to NRs and responsible for: (1) receptor dimerization; (2) ligand recognition and (3) cofactor interaction.



**Figure 1.** Schematic diagrams for a common domain structure of NRs which include N-terminal activation function 1 (AF-1), DNA binding domain (DBD) consisting of two zinc fingers (ZF), non-conserved hinge-region (Hinge), ligand binding domain (LBD), and C-terminal AF-2 helix.<sup>8</sup>

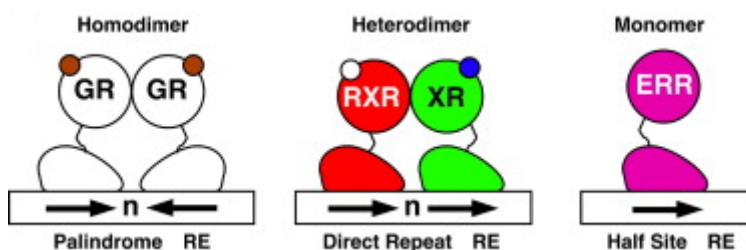


**Figure 2.** Schematic diagrams for NR dimerization and DNA binding sequences. From the left, homodimeric endocrine receptor (Palindrome RE), RXR heterodimers (Direct Repeat RE) and monomeric orphan receptor (Half Site RE). Arrows: the consensus NR recognition sequence AGGTCA or a variant.<sup>8</sup>

## 2. Nuclear Receptors subtypes

The NRs can be broadly classified into three sub-groups based on their physiologic ligands and potential functions (Figure 3). The first class comprises endocrine receptors which act as high affinity receptors for fat-soluble hormones and vitamins ( $K_d = \text{nM}$

range). This class includes receptors for the steroid hormones, thyroid hormone (thyroid hormone receptor; TR), and vitamins A (retinoic acid receptors; RAR) and D (vitamin D receptor; VDR), which are all essential for homeostatic control of the endocrine system. Mechanistically, the steroid receptors function as homodimers and TR, VDR, and RAR form heterodimers with the Retinoid X Receptor (RXR).

## Human Nuclear Hormone Receptor Superfamily

Endocrine Receptor	Adopted orphan receptor	Orphan Receptor
<b><u>Steroid Receptor</u></b> GR      Glucocorticoids MR Mineralocorticoids PR      Progesterone AR      Androgens ER $\alpha,\beta$ Estrogens	<b><u>Lipid Sensors</u></b> PPAR $\alpha,\beta,\gamma$ Fatty acids RXR $\alpha,\beta,\gamma$ 9cRA LXR $\alpha,\beta$ Oxysterol FXR      Bile acids PXR      Xenobiotics	SHP      ? DAX-1      ? TLX      ? PNR      ? GCNF      ? TR2,4      ? NRA4 $\alpha,\beta,\gamma$ ? Rev-erb $\alpha,\beta$ ? COUP $\alpha,\beta,\gamma$ ?
<b><u>Heterodimeric Receptors</u></b> TR $\alpha,\beta$ Thyroid hormone RAR $\alpha,\beta,\gamma$ Retinoic acid VDR      Vitamin D(bile acid)	<b><u>Enigmatic Receptors</u></b> CAR      Androstane HNF-4 $\alpha,\gamma$ Fatty acid SF-1/ LRH-1 Phospholipids ROR $\alpha,\beta,\gamma$ Cholesterol & Retinoic acid ERR $\alpha,\beta,\gamma$ Estrogen??	

**Figure 3.** Human NR superfamily including 48 family members. Representative natural ligands are shown at right. Physiological importance of ligand-induced NR activation has been established for “Endocrine Receptors” (Purple: homodimerizing steroid receptors, and Red: RXR heterodimers); “Adopted Orphan Receptors” (Orange); “Enigmatic Adopted Orphans” (Blue); and “Orphan receptors” (Grey).<sup>8</sup>

The second receptor class is the adopted orphans, which were originally identified based on sequence homology to endocrine receptors. These receptors were previously classified as orphans as no known natural ligands were identified, but later “de-orphanized” by subsequent identification of naturally occurring ligands. Identification of a vitamin A derivative, 9-*cis* retinoic acid, as an endogenous high-affinity ligand for RXR represented the first true adoption of an orphan NR and ushered in the age of “reverse endocrinology” in which a receptor is used to discover its natural ligand.<sup>9</sup> This class now includes low affinity ( $K_d = \mu\text{M}$  range) receptors for dietary lipids and xenobiotics, which all function as heterodimers with RXR. Some RXR heterodimers can be activated by RXR ligands (permissive) but others cannot (non-permissive).<sup>10</sup> Included within adopted orphans are “enigmatic” adopted orphans, for which a ligand has been identified, at least for one of the subtypes, but the nature of ligand-dependent regulation in physiology has not been established. Receptors of this class are the most promising drug targets for metabolic disorders as they regulate lipid and/or glucose homeostasis by controlling uptake, synthesis, storage or clearance.

The third class of NRs comprised of true orphans whose ligand (natural or synthetic) has not been identified. This class includes receptors which are most likely not regulated by ligands based on the size of the ligand binding pocket and the position of AF-2 helix in the apo-form in X-ray crystal structures (NR4A).<sup>11</sup> Most likely they are regulated by coactivator availability, receptor expression itself, covalent modification or a combination of all of these. This class of orphan receptors has attracted considerable interest since they could lead to the discovery of new endocrine regulatory systems.

Since transcriptional activity of many NRs can be modulated by lipophilic ligands, and in turn NRs control fundamental processes important for metabolic and energy homeostasis, NRs provide a powerful platform for drug discovery to treat metabolic disease. Indeed, a number of synthetic ligands for endocrine receptors as well as adopted orphan receptors are currently in clinical use or under clinical trial (Table 1).<sup>8</sup> In addition to the receptors that we described here, there are a number of orphan receptors about which little is known. As an obesity pandemic and associated illnesses such as type-2 diabetes and cardiovascular disease spread around the globe, particular attention has been focused on the role of NRs in the pathophysiology and/or treatment of metabolic diseases including the metabolic syndrome. Here, we review the current understanding of NR biology in the context of metabolic regulation and disease.



**Table 1.** NRs associated with metabolic disease, and their synthetic ligands

<b>Receptor (or coactivator)</b>	<b>Associated metabolic disease or pathologies</b>	<b>Synthetic ligand or modulator being used to ameliorate metabolic disease</b>	<b>Other representative synthetic ligands</b>
<b>GR</b>	Visceral obesity, hyperglycemia	N/A	Dexamethasone, RU38486
<b>MR</b>	Hypertension	Aldosterone antagonist (Spironolactone, Eplerenone)	Fludrocortisone
	Cardiac failure		
<b>TR<math>\beta</math></b>	Hypercholesterolemia	N/A	GC-1, KB-141
<b>PPAR<math>\alpha</math></b>	Dyslipidemia	Fibrate (Gemfibrozil, fenofibrate, clofibrate)	WY14643
	Atherosclerosis		
<b>PPAR<math>\gamma</math></b>	Diabetes Mellitus, insulin-resistant	Thiazolidinedione (pioglitazone, rosiglitazone)	FMOC-L-Leucine
	Atherosclerosis		
<b>PPAR<math>\delta</math></b>	Dyslipidemia	N/A	GW501516, KD3010
	Atherosclerosis		
<b>LXR<math>\alpha/\beta</math></b>	Dyslipidemia atherosclerosis	N/A	T0901317, GW3965
<b>FXR</b>	Hypercholesterolemia	Guggulsterone (antagonist)	Fexaramine, GW4046
	Biliary cholestasis	Chenodeoxycholic acid (agonist)	
	Dyslipidemia		
<b>PXR</b>	Biliary cholestasis, jaundice	St. John's wort (hyperforin), rifampin	SR12813
<b>CAR</b>	Biliary cholestasis, jaundice	Yin Zhi Huang (6,7-dimethylesculetin)	CITCO
<b>ERR<math>\alpha/\gamma</math></b>	Insulin resistance	N/A	XCT790, 4-hydroxytamoxifen
<b>HNF4<math>\alpha</math></b>	MODY, type I Non-insulin dependent diabetes mellitus	N/A	N/A
<b>SHP</b>	Mild obesity	N/A	N/A
<b>ROR<math>\alpha</math></b>	Atherosclerosis	N/A	

### 3. Estrogen Receptor

The estrogen receptor (ER) is a member of the nuclear hormone family of intracellular receptors which is activated by the hormone 17 $\beta$ -estradiol (estrogen). ER functions as a DNA binding transcription factor to regulate gene expression. However the estrogen receptor also has additional functions independent of DNA binding.<sup>12</sup> There are two different forms of ER, usually referred to as  $\alpha$  and  $\beta$ , each encoded by a separate gene (ESR1 and ESR2 respectively). Hormone activated estrogen receptors form dimers, and since the two forms are co-expressed in many cell types, the receptors may form ER $\alpha$  ( $\alpha\alpha$ ) or ER $\beta$  ( $\beta\beta$ ) homodimers or ER $\alpha\beta$  ( $\alpha\beta$ ) heterodimers.<sup>13</sup> Estrogen receptors alpha and beta show significant overall sequence homology, and both are composed of seven domains from the N- to the C-terminus.

Different ligands may differ in their affinity to the alpha and beta isoforms of the estrogen receptor. The natural ligand 17 $\beta$ -estradiol binds equally well to both receptors. Another natural ligand Estrone and synthetic ligand raloxone bind preferentially to the alpha receptor. The natural ligand Estriol and synthetic ligand genistein have more affinity for the beta receptor. The different estrogen receptor combinations may respond differently to various ligands which may translate into tissue selective agonistic and antagonistic effects. The ratio of  $\alpha$ - to  $\beta$ - subtype concentration has been proposed to play a role in certain diseases.<sup>14</sup>

The concept of selective estrogen receptor modulators is based on the ability to promote ER interactions with different proteins such as transcriptional coactivator or corepressors. These coactivator or corepressor regulates ERs transcriptional activity by

affecting the chromatin structure through the acetylation or deacetylation of histones, respectively. Estrogen receptor-mediated transcriptional activation is associated with the recruitment of coactivators, such as AIB1, GRIP1, SRC-1, CBP, p300, and pCAF, and subsequent histone acetylation. In contrast, antagonist-liganded ER is able to recruit corepressors. Furthermore the ratio of coactivator to corepressor protein varies in different tissues.<sup>15</sup> As a consequence, the same ligand may be an agonist in some tissue (where coactivators predominate) while antagonistic in other tissues (where corepressors dominate). Tamoxifen, for example, is an antagonist in breast and is therefore used as a breast cancer treatment but an ER agonist in bone (thereby preventing osteoporosis) and an agonist in the endometrium (increasing the risk of uterine cancer).<sup>16</sup> However the subcellular localization and roles of this receptor is still object of controversy.

#### **4. Peroxisome Proliferator-Activated Receptors (PPARs)**

The peroxisome proliferator-activated receptors (PPARs) are another group of nuclear receptor proteins that function as ligand-activated transcription factors regulating the expression of genes. PPARs play essential roles in the regulation of cellular differentiation, development, and metabolism (carbohydrate, lipid, and protein) of higher organisms. PPAR- $\alpha$  (NR1C1) (Nuclear Receptor Nomenclature Committee, 1999) was first described as a receptor that is activated by peroxisome proliferators, hence its name.<sup>17</sup> Two additional related isotypes, PPAR- $\beta/\delta$  (NR1C2) and PPAR- $\gamma$  (NR1C3) were then found and characterized. The PPAR- $\beta/\delta$  isotypes was called PPAR- $\beta$  when it was first isolated from a *Xenopus* oocyte library.<sup>18</sup> The PPAR- $\gamma$  gene was cloned from vertebrates, including

*Xenopus sp.*, mouse, and humans.<sup>18-20</sup> PPAR- $\beta$  protein sequences were not highly homologous to the *Xenopus* PPAR- $\beta$  protein sequences, and were subsequently named PPAR- $\delta$  when identified in the mouse.<sup>21</sup> PPAR- $\beta$  was also designated FAAR (fatty acid activated receptor) in rats and NUC1 in humans.

In humans, four different subtypes of PPAR- $\gamma$  mRNA ( $-\gamma 1$ ,  $-\gamma 2$ ,  $-\gamma 3$ , and  $-\gamma 4$ ) transcribed from four different promoters have been identified.<sup>22-24</sup> Despite four distinct mRNA subtypes, PPAR- $\gamma$  is expressed as two isoforms,  $\gamma 1$  and  $\gamma 2$  that differ at their N terminus. PPAR- $\gamma 2$  is found at high levels in the different adipose tissues, whereas PPAR- $\gamma 1$  has a broader expression pattern that extends to settings such as the gut, brain, vascular cells, and specific kinds of immune and inflammatory.

## **5. Transcriptional Regulation by PPAR- $\gamma$**

Differential promoter usage and alternate splicing of the gene generate three mRNA isoforms: PPAR- $\gamma 1$  and PPAR- $\gamma 3$  mRNA encode the same protein product; the PPAR- $\gamma 2$  isoform contains an additional 28 amino acids at its N-terminus. PPAR- $\gamma 1$  exhibits widespread expression, albeit at low levels, whilst PPAR- $\gamma 2$  is highly expressed in adipose tissue. Indeed, the receptor plays a critical role in fat cell differentiation, inducing the expression of adipocyte-specific genes, and promoting the formation of mature lipid-laden adipocytes.<sup>25, 26</sup> Recent studies with mice genetically engineered to lack PPAR- $\gamma$  have confirmed its critical role in the development of both white and brown adipocytes *in vivo*, and the clinical phenotypes of subjects with PPAR- $\gamma$  gene mutations suggest a similar role in the regulation of human adipose tissue mass.<sup>27-29</sup>

In contrast to steroid hormone receptors, which act as homodimers, transcriptional regulation by PPARs requires heterodimerization with the retinoid X receptor (RXR; NR2B).<sup>30, 31</sup> This PPAR/RXR heterodimer can form in the absence of a ligand. When activated by a ligand, it modulates transcription via binding to a specific DNA sequence element frequently called a peroxisome proliferator response element (PPRE). PPAR and RXR bind to the 5' and 3' half-sites of this element, respectively, and the 5'-flanking region mediates the selectivity of binding between different PPAR isotypes.<sup>32</sup> The transcriptional control by PPAR/RXR heterodimers requires interaction with coregulator complexes—either a coactivator for stimulation or a corepressor for inhibition of target gene expression.<sup>33</sup> Selective action of a given PPAR isotype *in vivo* probably results from a complex interplay at a given time point between expression levels of each of the three PPAR and RXR isotypes, affinity for a specific promoter PPRE, ligand and cofactor availability, and possibly binding of other transcription factor in the vicinity of the PPRE.<sup>34</sup>

The gene transcription mechanism is similar to that of all NRs, as shown in Figure 4.<sup>35</sup> In general, the C-terminal A/F domain of the receptor heterodimerizes with RXR- $\alpha$  and the PPAR/RXR- $\alpha$  complex binds to the PPRE sequence of the target gene promoters.<sup>30, 36, 37</sup> The PPRE motif contains a characteristic 13-nucleotide sequence, AGGTCA N AGGTCA (N – any nucleotide) that is composed of two hexanucleotides separated by one nucleotide (this type of sequences is called DR-1). The direct repeat 1 (DR-1) sites are specifically and almost exclusively recognized by the PPAR- $\gamma$ /RXR- $\alpha$  heterodimer. Each component of the heterodimer complex binds to one hexamer of the DR-1 motif. The unactivated PPAR- $\gamma$  is associated with a corepressor that silences its transcriptional activity by the recruitment

of histone deacetylases, such as the NR corepressor, the silencing mediator of retinoid and thyroid receptors (repression step). The binding of exo- or endogenous ligand to the receptor stimulates the release of the corepressor and the recruitment of a coactivator, which contains a protein with histone acetyl transferase (HAT) activity such as CREB (cAMP response element binding protein) binding protein (CBP/p300) or SRC-1 (derepression step). The action of acetyltransferases leads to chromatin decondensation. Following, the HAT complex dissociates and either transcription factors or the RNA polymerase II initiation complex are recruited to the accessible promoter, resulting in transcription activation of the target gene (transcription activation step). Interactions of PPAR- $\gamma$  with a coactivator or corepressor thus regulate its transcriptional activity by affecting the chromatin structure through the acetylation or deacetylation of histones, respectively.

It should be mentioned that both coactivators and corepressors are highly versatile and are not selective for particular PPAR subtypes. It has been observed, for example, that all three members of the PPAR family are subjected to transcriptional coactivation by the PPAR- $\gamma$  coactivator-1 $\alpha$  (PGC-1 $\alpha$ ), which is highly expressed in tissues with high mitochondrial metabolism, such as brown adipose tissue, heart, and skeletal muscle.<sup>33, 38-40</sup>

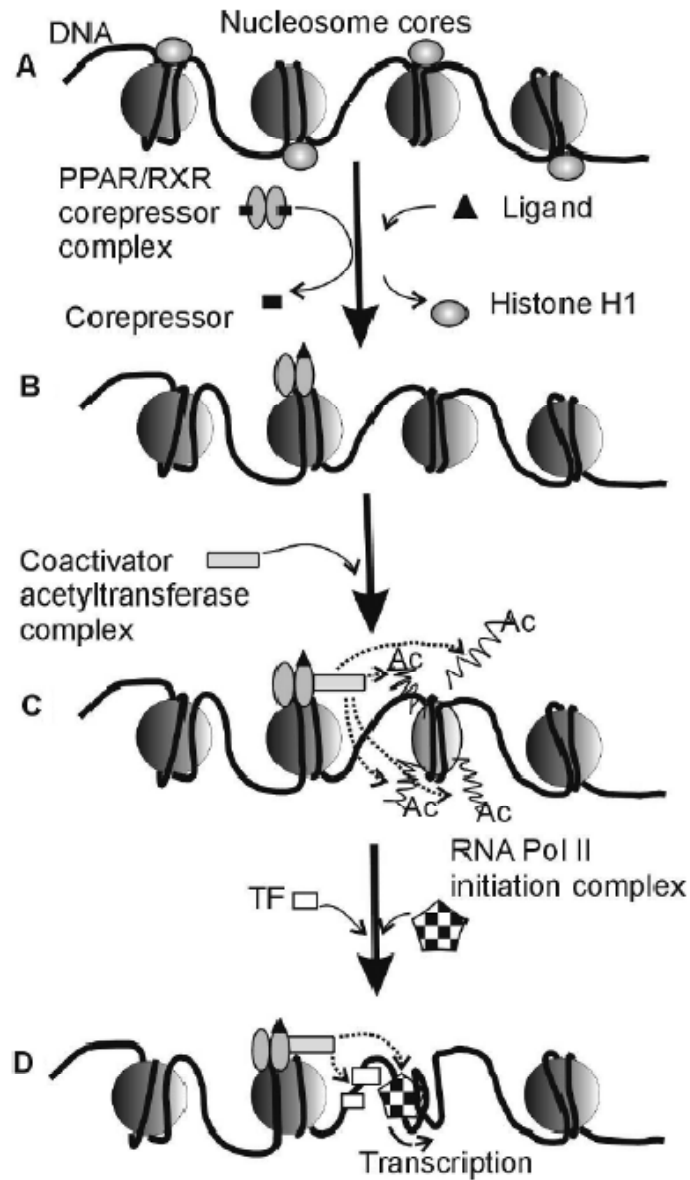


**Figure 4.** Transcriptional activity of PPARs. (A) The promoter region with a PPRE, the TATA box, and the transcription start site is located in a repressive chromatin structure. The binding of ligand to the PPAR/RXR/corepressor complex causes the release of the corepressor from the ligand-activated PPAR/RXR complex. (B) The activated PPAR/RXR complex binds to the PPRE, inducing structural change in chromatin, with histone H1 released. The PPRE-bound PPAR/RXR targets a coactivator-acetyltransferase complex to the promoter. (C) The coactivator-acetyltransferase complex acetylates the histone tails (Ac), thereby generating a transcriptionally active structure. (D) Additional transcription factors (TF) and the RNA Pol II initiation complex are recruited to the accessible promoter and transcription is initiated.<sup>35, 41</sup>

## 6. Functional and Medicinal Roles of PPARs

As noted above, there are three different PPAR isotypes namely PPAR- $\alpha$ , - $\delta$ , and - $\gamma$ , which have been identified in vertebrates and have distinct pattern of distribution. PPARs are important targets for the drugs used in the treatment of atherosclerosis, dyslipidaemia, obesity, diabetes, and other disease caused by abnormal regulation of glucose and lipid metabolism.

PPAR- $\alpha$  is distributed in tissues with high catabolic rates of fatty acids and high peroxisomal activity, and the major role of PPAR- $\alpha$  is the regulation of energy homeostasis.<sup>42</sup> In liver, PPAR- $\alpha$  activates fatty acid catabolism, stimulates gluconeogenesis and ketone body synthesis, and is involved in the control of lipoprotein assembly.<sup>43</sup> PPAR- $\alpha$  also stimulates heme synthesis, cholesterol catabolism, attenuates inflammatory responses, and participates in the control of amino acid metabolism and urea synthesis. Increased fatty acid oxidation by activated PPAR- $\alpha$  lowers circulating triglyceride levels, liver and muscle steatosis, and reduces adiposity, which improves insulin sensitivity.<sup>44</sup> The fibrate drugs such as gemfibrozil, clofibrate, and fenofibrate that are widely used to treat hypertriglyceridemia are activators of PPAR- $\alpha$ . In addition, PPAR- $\alpha$  agonists have demonstrated significant anti-inflammatory activities that seem to play a role in their protective actions within the cardiovascular system.<sup>45</sup>

PPAR- $\delta$  is necessary for placental and gut development and is also involved in the control of energy homeostasis by stimulating genes involved in fatty acid catabolism and adaptive thermogenesis.<sup>46, 47</sup> In addition, PPAR- $\delta$  has an important role in the control of cell proliferation, differentiation, and survival and is involved in tissue repair.<sup>48</sup> In animal



models, PPAR- $\delta$  agonists retard weight increase under high-fat diet conditions and therefore maintain insulin sensitivity probably by stimulating skeletal muscle fatty acid metabolism and thermogenesis.<sup>40</sup>

PPAR- $\gamma$  is a pivotal actor in adipose tissue differentiation and in maintaining adipocyte specific functions, such as lipid storage in the white adipose tissue and energy dissipation in the brown adipose tissue.<sup>49, 50</sup> In addition, PPAR- $\gamma$  is involved in glucose metabolism through an improvement of insulin sensitivity and thus represents a molecular link between lipid and carbohydrate metabolism. Like PPAR- $\alpha$ , - $\gamma$  activation seems to limit inflammation, adding to the interest in its possible role in limiting atherosclerosis and/or diabetes.<sup>51, 52</sup> Among the synthetic compounds that selectively activate PPAR- $\gamma$ , the thiazolidinediones (TZDs) are insulin sensitizers used to treat the hyperglycemia of type 2 diabetes.<sup>53, 54</sup> The clinical use of these agonists and the discovery of both rare and severely deleterious dominant-negative mutations that lead to a stereotyped syndrome of partial lipodystrophy and severe insulin resistance, as well as more common sequence variants with a much smaller impact on receptor function, have increased our understanding of the functions of PPAR- $\gamma$  in humans.<sup>55</sup> Finally, growing evidence implicates PPAR- $\gamma$ , as well as the two other isotypes, in tumor development in different tissues, although whether PPAR activation promotes or limits this process remains under debate and may depend on specific conditions.<sup>56, 57</sup>

## **7. Structure of PPAR**

All three PPAR isotypes have a protein domain organization similar to most members of the superfamily (Figure 1A). This includes the NH<sub>3</sub>-terminal region, the central DNA-binding domain (DBD), the hinge region, and the C-terminal ligand-binding domain (LBD). The best-characterized domains are the DBD and LBD. Although the latter is generally less well conserved than the former, X-ray crystal structure analyses have revealed a three dimensional fold of the PPAR LBD that is similar to other nuclear receptors.

The N-terminal domain A/B has been relatively well conserved through evolution. The chief fragment of this domain is  $\alpha$ -helix fragment possessing a ligand-independent activating function (AF-1). It has been shown that the hPPAR- $\gamma$ 2 isoform exhibits tenfold higher activity than hPPAR- $\gamma$ 1 in the presence of insulin in ligand-independent transcriptional activation.<sup>58</sup> This data may imply different functions of the two isoforms that differ only in their N-termini. So far, the role of the additional 28 amino-acid residues at the N-terminus of the hPPAR- $\gamma$ 2 protein has not been explained. However, there are some hypotheses about this fragment concerning its effect on an increase in receptor activity.<sup>59</sup> Furthermore, in the A/B domain is Ser112, which is subject to phosphorylation. Since intramolecular communication between the A/B and the LBD domains is required for ligand binding, the phosphorylation at Ser112 by mitogen-activated protein kinase (MAPK) disrupts interdomain communication, resulting in a reduction in ligand-binding affinity.<sup>60</sup> Moreover, the MAPK-dependent phosphorylation of this residue in the hPPAR- $\gamma$ 2 protein inhibits its ability to promote specific gene expression and the process of adipogenesis.<sup>61</sup>

The C domain is the most conserved of all the functional domains. It contains two zinc finger-like motifs that are responsible for binding of the receptor to the DNA promoter of target genes. Each of the zinc fingers is encoded by a separate exon (2 and 3). Besides the zinc fingers there are amino-acid motives determining the recognition of an appropriate DNA sequence which binds the receptor. Additionally, a large part of the domain takes part in dimerization with another nuclear receptor, RXR.

The less conserved domain D is a flexible hinge between the C and E/F domains.<sup>35</sup> This site is also a docking domain for cofactors. In addition, it contains the nuclear localization signal, a sequence recognized by transporting proteins, which determines relocation of the synthesized protein from the cytoplasm to the cell nucleus. Moreover, some of the amino acids are involved in the activities of both nearby domains, leading to the dimerization and recognition of the target DNA sequence.

## **8. Ligand Binding Domain**

The largest structural domain of PPAR is the LBD (E/F domain) located at the C-terminus, and responsible for the binding of a specific ligand and activation of PPAR binding to PPRES in the target gene promoter. The PPAR LBD consists of 12  $\alpha$ -helices that form the characteristic three-layer anti-parallel  $\alpha$ -helical sandwich with a small four-stranded sheet. This structure delineates a large Y-shape hydrophobic pocket, the ligand-binding cavity, which is larger in PPARs than in other receptors.<sup>62, 63</sup> This feature may contribute to the ability of PPARs to bind a wide range of synthetic and natural lipophilic compounds with an acidic head group. Comparison of the ligand-binding pocket of the

three PPAR isotypes has revealed the following interesting characteristics.<sup>64</sup> The PPAR- $\delta$  ligand-binding pocket is significantly smaller than the corresponding PPAR- $\alpha$  and PPAR- $\gamma$  pockets, which are similar to each other in shape and size. This difference might explain why fewer PPAR- $\delta$  ligands have been reported compared with PPAR- $\alpha$  and PPAR- $\gamma$  and may indicate that the size of the pocket contributes to the ligand-binding specificity of this isotype. The PPAR- $\alpha$  pocket is more lipophilic than the two others, which suggests a possible explanation for why certain potent PPAR- $\gamma$  ligands do not bind PPAR- $\alpha$  and why PPAR- $\alpha$  can bind the more lipophilic-saturated fatty acids. Finally, it is important to note that single amino acid differences in the pockets can be major determinants of ligand isotype selectivity.

The LBD contains a fragment called ligand- dependent activation function 2 (AF-2), engaged in the recruitment of PPAR cofactors to assist the gene transcription processes.<sup>62,</sup>  
<sup>65</sup> Ligand-dependent activation of PPAR stabilizes the LBD in a relatively compact and rigid structure in which helix 12 is in a confirmation that promotes binding of coactivator proteins and thus has a critical function in the stimulation of target genes.<sup>62, 66</sup> Examples of coactivators are CBP/p300 and steroid receptor coactivators (SRC-1), PGC-1, RIP140, ARA70. Usually nucleosome remodeling, for example by histone deacetylation and repositioning, is necessary to allow formation of the transcription preinitiation complex. Alternatively, corepressors inhibit the activity of the receptors in the absence of a ligand or upon antagonist treatment. Examples of corepressors are SMRT and NCOR. Often, the repressive effects depend on the recruitment of histone deacetylases, but sometimes direct contacts with the basal transcription machinery are also possible.<sup>67, 68</sup>

A “mouse trap” model of receptor activation has been proposed. According to this model, helix 12, containing the conserved AF-2 core, closes the ligand binding site in response to a bound ligand, resulting in a transcriptionally active form of the receptor.<sup>69</sup> The recently solved X-ray structure of the PPAR- $\gamma$ /RXR $\alpha$  LBD heterodimer in complex with a synthetic ligand, GW409544 and two LXXLL (L, leucine; X, any amino acid) peptides from SRC-1 revealed that the acidic head group of GW409544 forms hydrogen bonds with either His-323 (helix 5) or Tyr-473 (the AF2 helix) within PPAR- $\gamma$ . In addition, comparison of the structures of GW409544 bound to PPAR- $\alpha$  and PPAR- $\gamma$ , along with mutational analysis of their LBDs, resulted in the identification of the single amino acids which determine ligand selectivity. These are Tyr-314 in PPAR- $\alpha$  and His-323 in PPAR- $\gamma$ , which constitute part of the network of hydrogen-binding residues involved in the activation of PPAR through its acidic ligands.<sup>64</sup> It is noteworthy that the identification of a major determinant of selectivity between PPAR- $\alpha$  and PPAR- $\gamma$  has provided the opportunity to design new diabetes drugs. Currently however, synthetic ligands like TZDs and tyrosine agonists remain the most potent known activators of PPAR- $\gamma$ .<sup>70</sup>

The crystal structure of the apo-PPAR- $\gamma$  LBD reveals a bundle of 13  $\alpha$ -helices and a small four-stranded  $\beta$ -sheet (Figure 5). The PPAR- $\gamma$  LBD is very similar to the overall fold of other nuclear-receptor structures from helix 3 to the C terminus. However, PPAR- $\gamma$  is unique in its overall tertiary structure and contains an extra helix, designated H29, between the first beta-strand and helix H3. The tertiary placement of helix H2 is different in PPAR- $\gamma$  compared with other nuclear-receptor LBD tertiary structures, and provides easier access for ligands. Helices H4, H5 and H8 are tightly packed between helices H1, H3, H7 and

H10 at the top half of the LBD. This structural arrangement seems to be important in forming the ligand-binding site: helices H3, H7 and H10 are anchored to allow them to jut downwards and form the scaffolding for the large cavity of the ligand-binding site in PPAR- $\gamma$ . The binding cavity of the apo-PPAR- $\gamma$  LBD site is T-shaped and extends from the C-terminal helix to the  $\beta$ -sheet lying between helices H3 and H6. This domain is mainly hydrophobic and is buried within the bottom half of the LBD. One region of the domain is 20Å in length, lies between helix H3 and the  $\beta$ -sheet, and is parallel to helix H3. Another cavity, which extends from the  $\beta$ -sheet to the C-terminal AF-2 helix and is 16 Å in length, is orthogonal to the T-shaped cavity, behind helix H3.<sup>62</sup>

The crystal structure of PPAR- $\gamma$  LBD in complex with the TZD, Rosiglitazone and co-activator, SRC-1 has been elucidated, and shows Rosiglitazone to occupy roughly 40% of the ligand-binding site in the ternary complex (Figure 6). In general the ligand is in a U-shaped conformation, wrapping around helix H3 with its central benzene ring directly behind H3 and the thiazolidinedione head group and pyridine ring wrapping around helix H3. The thiazolidinedione head group makes several specific interactions with amino acids in helices H3, H4, H10 and the AF-2 helix (Figure 6). The carbonyl groups of the TZD form hydrogen bonds with two histidine residues, H323 and H449. Y473 in the AF-2 helix forms a secondary hydrogen-bond interaction with H323. The partly negatively charged nitrogen of the TZD head group is within hydrogen-bonding distance of the Y473 side chain hydroxyl group. A buried lysine residue, K367, forms another secondary hydrogen-bond interaction with the ligand mediated by residue H449. All of these primary and secondary hydrogen-bond interactions result in a fixed conformation of the

thiazolidinedione head group and of the participating amino acids. Next to the head group, the sulfur atom of the thiazolidinedione ring is positioned in a hydrophobic region of the PPAR- $\gamma$  ligand-binding pocket formed by F363, Q286, F282 and L469. The central benzene ring of the ligand occupies a very narrow pocket between C285 and M364. The bridging oxygen atom between the benzene ring and the pyridine ring provides vital geometry for the pyridine ring, which occupies the pocket between helix H3 and the  $\beta$ -sheet.

## **9. Rationale and Hypothesis**

PPAR- $\gamma$  plays a vital role in adipose tissue differentiation.<sup>71</sup> In addition, PPAR- $\gamma$  is involved in glucose metabolism through an improvement of insulin sensitivity and thus represents a molecular link between lipid and carbohydrate metabolism.<sup>51, 72</sup> Like PPAR- $\alpha$ , PPAR- $\gamma$  activation seems to limit inflammation, adding to the interest in its possible role in limiting atherosclerosis and/or diabetes.<sup>52</sup> Among the synthetic compounds that selectively activate PPAR- $\gamma$ , the thiazolidinediones (TZDs) are insulin sensitizers used to treat the hyperglycemia of type 2 diabetes.<sup>53, 54, 73</sup> TZDs have been shown to selectively stimulate lipogenic activities in fat cells resulting in greater insulin suppression of lipolysis.<sup>74</sup> Two of these TZD, Rosiglitazone and Pioglitazone are clinically approved for the treatment of type 2 diabetes mellitus and offer a new approach in the pharmacologic management of this disease. Unlike other oral antidiabetic agents, TZDs are unique because they improve insulin sensitivity by increasing insulin-mediated glucose uptake in skeletal muscle, suppressing hepatic glucose output and improving the secretory response of insulin in

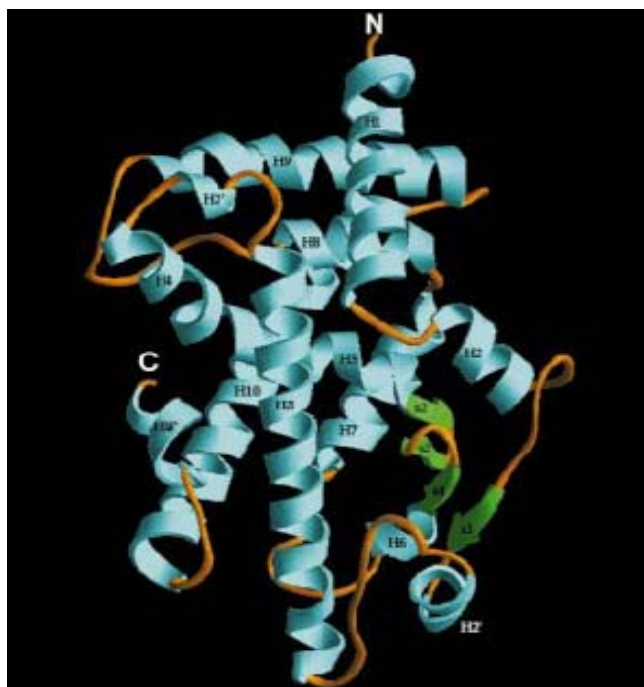


**Figure 5.** Crystal structure of the apo-PPAR- $\gamma$ .<sup>62</sup>

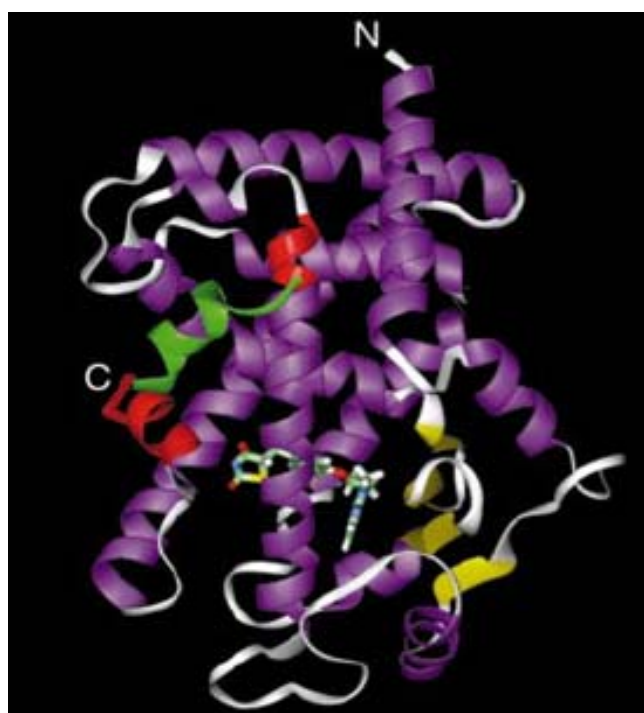


**Figure 6.** Crystal structure of PPAR- $\gamma$  LBD in complex with Rosiglitazone.<sup>62</sup>



pancreatic  $\beta$ -cells. The findings that TZDs could form a number of reactive intermediates, including quinones and quinone methides, led investigators to hypothesize that TZDs hepatotoxicity was mediated by these intermediates through either a classic Glutathione (GSH) depletion/covalent binding mechanism or via oxidative stress caused by redox cycling of the quinone. This would potentially explain the zone 3 centrilobular necrosis produced by TZDs in the liver as P450 activities are higher and GSH levels are lower in this zone than in others. Quinones are also well-established cytotoxic agents and can produce toxicity by redox cycling with molecular oxygen to produce superoxide anion radical and subsequent oxidative stress.<sup>75</sup>

The TZDs are indicated in the United States for monotherapy and as combination therapy with sulfonylureas, metformin and insulin for treatment of type 2 diabetes mellitus.<sup>76, 77</sup> As monotherapies, both Rosiglitazone and Pioglitazone significantly improve insulin sensitivity and glycemic control in type 2 diabetes mellitus patients by decreasing plasma glucose and plasma insulin levels, thus reducing HbA1c levels from 0.5% to 1.9%.<sup>78, 79</sup> In combination therapy with other oral diabetes medications, both Rosiglitazone and Pioglitazone demonstrate additive effects on glycemic control compared with monotherapy.<sup>76</sup>

After studying the crystal structure of Rosiglitazone in the binding pocket of PPAR- $\gamma$  LBD with the co-activator SRC-1,<sup>62</sup> we decided to design novel PPAR- $\gamma$  agonistic ligands based on the mode of Rosiglitazone interactions with PPAR- $\gamma$  LBD.

The objective is to take advantage of the PPAR- $\gamma$  LBD binding site characteristics and the mode of binding of known PPAR- $\gamma$  agonists to rationally design novel agonists of

PPAR- $\gamma$ . The goal is to generate new and potent PPAR- $\gamma$  agonists that could be used to treat diabetes. Our working hypothesis is that these compounds will bind to PPAR- $\gamma$  LBD and exhibit agonistic effects. To achieve our goal the study was divided into five specific aims:

**Aim 1.** Expression and purification of PPAR- $\gamma$  LBD.

**Aim 2.** Molecular modeling to design PPAR- $\gamma$  receptor modulators.

**Aim 3.** Synthesis of potential PPAR- $\gamma$  receptor modulators.

**Aim 4.** Functional studies to determine the binding affinity of PPAR- $\gamma$  receptor modulators.

**Aim 5.** Structural studies of PPAR- $\gamma$  LBD in complex with PPAR- $\gamma$  receptor modulators.

## {CHAPTER II Experimental Methods}

### 1. Expression and Purification of PPAR- $\gamma$ LBD.

The plasmid containing the LBD fragment of the human PPAR- $\gamma$  (residues 195-477) and a pGEX-4T1 vector with GST gene (GE Healthcare) were digested with restriction enzymes *Bam*HI and *Xho*I, and then run on an agarose gel. The LBD fragment and the pGEX-4T1 vector were extracted from the gel using a Qiagen (Valencia, California) DNA extraction kit and then ligated with T4 DNA ligase (Novagen). The ligated plasmid was transformed into Rosetta (DE3) cells (Novagen), which were grown at 37°C in LB medium containing 50 $\mu$ g/ml kanamycin and 34 $\mu$ g/ml chloramphenicol, and after reaching an OD<sub>600nm</sub> of 1.0, it was induced with 1.0 mM isopropyl- $\beta$ -D thiogalactopyranoside (IPTG). Incubation was carried out in a mechanical shaker at 37°C for 18 hours (overnight). Cells were harvested with centrifugation and broken with Avestin EmulsiFlex-C3 homogenizer. The solution was saturated with ammonium sulfate to 20% and the precipitate discarded. Second ammonium sulfate treatment (45% saturation) yielded a precipitate with 98% of the activity of the lysate. Cells were collected by rapid centrifugation and resuspended in 1 X PBS (137 mM NaCl, 2.7 mM KCl, 4.3 mM Na<sub>2</sub>HPO<sub>4</sub>, 1.47 mM KH<sub>2</sub>PO<sub>4</sub>), pH 7.4, and 1 mM dithiothreitol (DTT) containing 1 mM phenylmethylsulfonyl fluoride and dialyzed overnight against the same buffer. The GST-PPAR fusion protein was purified from the

cell pellet using glutathione-sepharose beads, following the procedure recommended by the manufacturer (Amersham Pharmacia Biotech). The dialyzed protein was then centrifuged at 5,000 rpm, to remove some of the turbidity so that it does not clog the column. The protein was loaded on to a previously equilibrated GST-column with 1 X PBS buffer, and then washed with 200 ml of 1 X PBS buffer to remove extra non-bound protein. For removal of the GST moiety, we digested the fusion protein with thrombin (Pharmacia) on the column. The cleaved PPAR- $\gamma$  LBD was eluted with elution buffer (50 mM Tris-HCl, 10 mM reduced glutathione), pH 8.0. The protein yield was 5mg/L determined using Bradford assay. Due to poor expression, as well as time consuming and labor intensive purification procedure, an alternate method was developed (see below) for obtaining pure protein with better yield.

The plasmid containing the LBD fragment of the human PPAR- $\gamma$  (residues 204-477) amplified from a cDNA library from human fetal brain tissue (Invitrogen), was obtained from our Brazilian collaborators, Polikarpov and colleagues, and transferred to competent Rossetta cells (Strat-agene). The transformed cells were grown in Luria-Bertani medium containing 50 $\mu$ g/ml kanamycin and 34 $\mu$ g/ml chloramphenicol at 37°C. At OD<sub>600nm</sub> of 0.5, the expression was induced by addition of 0.1 mM IPTG for 18 hours (overnight) at 25°C. Cells were harvested with centrifugation and broken with Avestin EmulsiFlex-C3 homogenizer. Cell lysis was performed using lysozyme treatment followed by homogenization. After collecting the soluble fraction, the protein product was isolated in a single purification step by immobilized metal affinity chromatography using the Ni-nitrilotriacetic acid (NiNTA) column (Invitrogen), previously equilibrated with the

running buffer 50 mM NaCl, 25 mM Tris-HCl, pH 8.0. The PPAR- $\gamma$  LBD bearing a His-tag fused to its N terminus was eluted stepwise using running buffer to which up to 200 mM imidazole had been added. After purification, 5 mM DTT was added to the buffer. The purity of the protein was determined to be greater than 95% using SDS gel electrophoresis.

## **2. Molecular Modeling to Design PPAR- $\gamma$ Receptor Modulators.**

### **A. Design:**

Our purpose was to use the binding mode of Rosiglitazone in PPAR- $\gamma$  LBD to design potent agonists of this nuclear receptor. The molecular modeling program Sybyl, and the crystallographic modeling programs TOM<sup>80</sup> and COOT<sup>81</sup> were used for the design studies. The known crystal structure of PPAR- $\gamma$  LBD in complex with Rosiglitazone (PDB code 2PRG) was used as the docking model.

Figures 6 and 7 show the binding of Rosiglitazone to PPAR- $\gamma$  LBD (PDB code 2PRG). The carbonyl groups of the TZDs form hydrogen-bond interactions with the side-chains NE2 atoms of His323 and His449. The partly negatively charged nitrogen of the thiazolidinedione moiety is within hydrogen-bonding distance of the Tyr473 side chain hydroxyl group. The central benzene ring of the ligand occupies a very narrow pocket between Cys285 and Met364. Binding of ligand is believed to activate a nuclear receptor heterodimer, PPAR- $\gamma$ /RXR- $\alpha$  through covalent binding to Cys285 in PPAR- $\gamma$  LBD.<sup>82</sup> The bridging oxygen atom between the benzene ring and the pyridine ring provides vital

geometry for the pyridine ring, which occupies the pocket between helix H3 and the  $\beta$ -sheet.

Based on the binding mode of Rosiglitazone, we reasoned that increased affinity and agonistic activity of ligands to PPAR- $\gamma$  LBD can be obtained by exploiting some potential binding interactions as noted below.

1. The residue, Cys285 could be utilized to make potential hydrogen-bond interaction with the ligand.
2. There is a hydrophobic cavity formed by Ile281, Met348, Ile341 and Arg288 near the pyridine ring of Rosiglitazone, which can be utilized to make hydrophobic contact with the ligand.

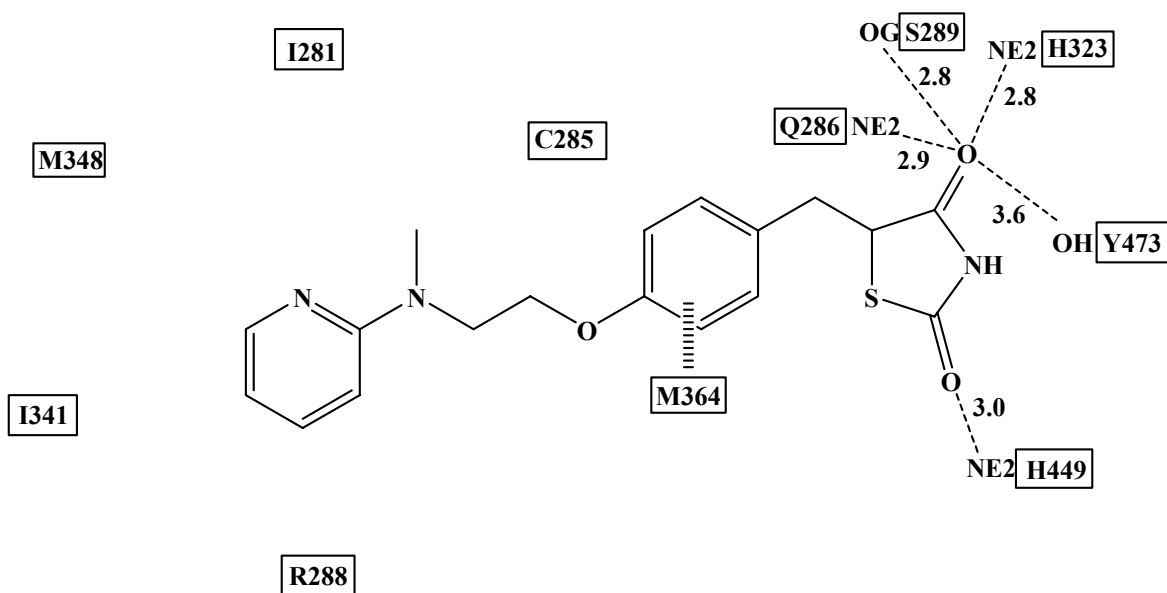
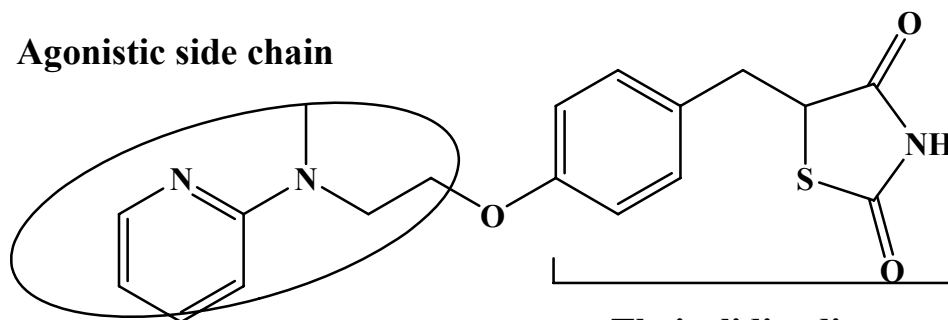


**Figure 7.** Rosiglitazone in crystal structure with PPAR- $\gamma$  LBD.

**A.**

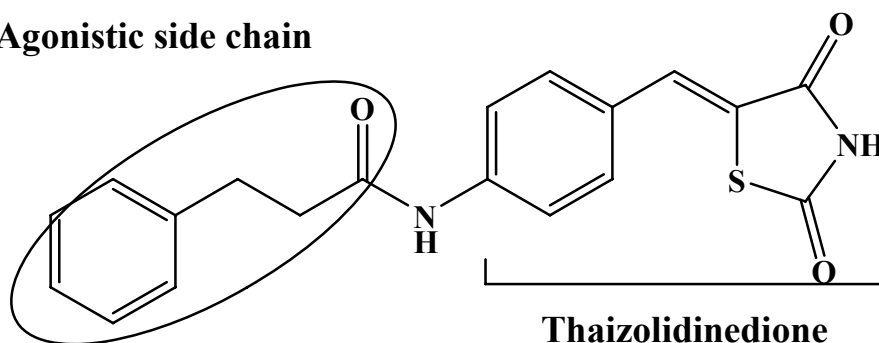
**Agonistic side chain**



**Thaizolidinedione  
core structure**

**B.**

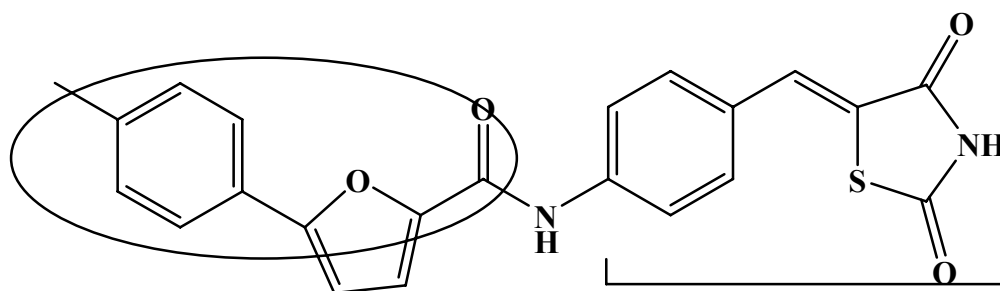
**Agonistic side chain**



**Thaizolidinedione  
core structure**

**Type-I compound**

**C. Agonistic side chain**



**Thaizolidinedione  
core structure**

**Type-II compound**

**Figure 8.** A. Structural components of PPAR- $\gamma$  LBD agonists. B. Structural design of type-I compounds. C. Structural design of type-II compounds.

Based on these assumptions, we identified two important parts of the Rosiglitazone structure – the thiazolidinedione core structure and the hydrophobic agonistic side-chain as shown in Figure 8A. Using these two identified pharmacophores, two classes of novel compounds can be designed. We will call these type-I and type-II compounds. For the type-I compounds, the ether bridge between the core structure and the hydrophobic side chain is modified as an amide without extending the hydrophobic chain length. An example of type-I compound (compound **A**) is shown in Figure 8B. This class of compounds is hypothesized to bind similarly as Rosiglitazone but with additional hydrogen-bond interaction between the amide oxygen of the ligand and Cys285 of PPAR- $\gamma$  LBD.

For type-II compounds, in addition to replacing the ether linkage with an amide moiety, the hydrophobic part is also extended by incorporating additional ring (isoxazole or furan) to the phenyl substituent. An example of type-II compound (compound **B**) is shown in Figure 8C. This compound is proposed to bind to increase both hydrogen-bond and hydrophobic interactions with the protein.

## **B. Docking:**

Using SYBYL 7.3, representative molecules of these two classes (compound **A** from type-I and **B** from type-II) were built and energy minimized. The crystallographic structure of PPAR- $\gamma$  LBD in complex with Rosiglitazone was obtained from the Protein Data Bank (PDB code 2PRG) and used as the target molecule for docking the minimized compounds **A** and **B**. Prior to docking the molecules into the target, hydrogen atoms which are not part of the 2PRG structure were added to the protein using tools within SYBYL 7.3. The added



hydrogen atoms were energy minimized to reduce steric clashes with the protein residues to a gradient of 0.005 using Gasteiger Hückel charges, a dielectric constant of 1.0, and a gradient of 0.005Kcal/mol Å with 10,000 iterations.

This ensures the ideal position and conformation for the added hydrogen atoms. The coordinates of all non-hydrogen atoms were not altered during the minimization and were kept fixed.<sup>83</sup> The individual software programs used for the studies are all incorporated in the molecular modeling and graphic program SYBYL 7.3 (Tripos Inc) software suite.

The molecules were then manually docked into the known crystal structure of PPAR- $\gamma$  LBD using TOM and/or COOT, and then energy minimized with a subset of the active site residues using SYBYL. A hot radius of protein-ligand subset of 6 Å, and surrounding radius of 12 Å were used for the computation. Other conditions specified for the minimization process include Gasteiger Hückel charges, dielectric constant of 1.0, a gradient of 0.005 and 10,000 iterations, whereas the coordinates of all other atoms outside the subset were kept fixed. As a control, we also energy minimized the crystallographically bound Rosiglitazone.

Subsequently, the docked molecules were subjected to HINT (eduSoft, LC) analysis, to analyze the interactions between the compounds and the protein. HINT uses a scoring function that employs empirically derived parameter  $\log P_{o/w}$  (partition coefficient for 1-octanol/water) - utilizing fragment rules of Hansch and Leo.<sup>84, 85</sup> The program calculates a score for each interaction between various atoms of the protein and ligand, and the cumulative score is termed as HINT score. A positive HINT score value indicates hydrophatically favorable contacts (hydrogen bonds, acid/base, and

hydrophobic/hydrophobic), while negative value indicates unfavorable contacts (acid /acid, base/base, and hydrophobic/polar). The factor  $\log P_{o/w}$  of a ligand or biological molecule is the sum of all the hydrophobic atomic constants for that molecule, and directly correlated with free energy. HINT score therefore reveals information not only about enthalpy but also entropy of the bimolecular complex.<sup>83, 86, 87</sup>

### 3. Synthesis of Potential PPAR- $\gamma$ Receptor Modulators.

<sup>1</sup>H-NMR (Proton Nuclear Magnetic Resonance) spectra were obtained on a Varian Gemini 300 MHz spectrometer and tetramethylsilane was used as an internal standard. Routine thin-layer chromatography (TLC) was performed on silica gel GHIF plates (250  $\mu$ , 2.5 x 10 cm; Analtech Inc., Newark, DE). Elemental analysis was performed by Atlantic Microlab, Inc.

#### A. Chemical Synthesis:

Based on the above design studies, we devised three synthetic schemes, Scheme 1 - 3 to synthesize type-I and -II compounds. In scheme 1, we synthesized 5-(4-Amino-benzylidene)-thiazolidine-2,4-dione or (**4**), which is the common starting material for type-I and -II compounds. Scheme 2 involves synthesis of type-I compounds, including **A**, **D**, **G**, **H** and **I**. Scheme 3 involves synthesis of a type-II compounds, including **B**, **C**, **F**, **J** and **K**. We note that even though attempts were made to synthesize compounds **G**, **H** and **I** from type-I and **J** and **K** from type-II (shown in schemes 2 and 3 in results and discussion part), we failed to obtain the end products. The proceeding synthetic procedures are those

for the compounds that we were able to synthesize, which are similar to the procedures used for synthesizing the failed compounds.

**a. Intermediates:**

5-(4-Amino-benzylidene)-thiazolidine-2,4-dione, 4:

In scheme 1, 5-(4-Amino-benzylidene)-thiazolidine-2,4-dione or **4** was synthesized using a two step reaction procedure.

In step 1, a mixture of 4-nitrobenzaldehyde, **1** (5.0g, 33 mmol), 2,4-thiazolidinedione, **2** (3.9 g, 33 mmol), piperidine (0.5 mL) and acetic acid (0.5 mL) in toluene (100 mL) was heated to reflux with Dean Stark apparatus for 16 hours. The mixture was cooled in ice, the precipitate filtered, and washed with cold toluene. The product was re-crystallized from methanol to yield 5-(4-nitro-benzylidene)-thiazolidine-2,4-dione, **3**, to yield 5.07 g (61%); <sup>1</sup>H NMR (CD<sub>3</sub>COCD<sub>3</sub>) δ 7.77-7.80 (m, 3H), 8.26-8.29 (m, 2H), 12.4 (br, H).

In step 2, to a stirring solution of **3** (3.0 g, 12 mmol) in ethanol (100 mL) was added tin (II) chloride (13.6g, 60 mmol) and the mixture heated to reflux for 2 hours. The reaction mixture was cooled and neutralized with sodium bicarbonate and the product extracted with ethyl acetate (3 x 200 mL). The organic layer was dried (MgSO<sub>4</sub>), filtered and evaporated at reduced pressure to yield of 1.4 g (53%); <sup>1</sup>H NMR (CD<sub>3</sub>COCD<sub>3</sub>) δ 6.1 (br, 2H), 6.8 (d, 2H, *J* = 8.7 Hz), 7.4 (d, 2H, *J* = 8.4 Hz), 12.3 (br, H).

**b. Synthesis of Type-I Compounds:**

In scheme 2, compounds **A** and **D** were synthesized as follows:

N-[4-(2,4-Dioxo-thiazolidin-5-ylidenemethyl)-phenyl]-3-phenyl-propionamide, **A**:

To a mixture of **4** (500 mg, 2.3 mmol), and triethylamine (0.92 mg, 9.2 mmol) in dichloromethane (30 mL) at 0° C and under nitrogen was added hydrocinnamoyl chloride, **5** (383 mg, 2.3 mmol,) in dichloromethane (30 mL) dropwise. After stirring at the same temperature for ten minutes, the mixture was further stirred at room temperature for 2 hr. The mixture was washed with dilute hydrochloric acid (2 x 30 mL), and aqueous sodium bicarbonate (2 x 30) followed by brine (30 mL). The organic layer was dried (MgSO<sub>4</sub>), filtered and evaporated at reduced pressure to yield 500 mg (61%). <sup>1</sup>H NMR (CD<sub>3</sub>COCD<sub>3</sub>) δ 2.7 (t, 2H, *J* = 7.8 Hz), 3.0 (t, 2H, *J* = 7.5 Hz), 7.2 (t, H, *J* = 4.8 Hz), 7.3 (d, 4H, *J* = 6.9 Hz), 7.7 (s, H), 7.8 (d, 2H, *J* = 6.9 Hz). Anal. calc. for C<sub>19</sub>H<sub>16</sub>N<sub>2</sub>O<sub>3</sub>S : C, 64.76; H, 4.58; N, 7.95; Found : C, 64.50; H, 4.65; N, 7.88.

N-[4-(2,4-Dioxo-thiazolidin-5-ylidenemethyl)-phenyl]-2-(pyridin-3-yloxy)-acetamide, **D**:

To a mixture of **4** (500 mg, 2.3 mmol), 3-pyridyloxyacetic acid or **6** (348 mg, 2.3 mmol), under nitrogen at room temperature was added 1-hydroxybenzotriazole hydrate (HOBt) (337.5 mg, 2.53 mmol) and N-(3-dimethylaminopropyl)-N-ethylcarbodiimide (DEC) (523 g, 2.76 mmol), in N,N-dimethylformide (DMF) and the mixture stirred overnight. The reaction mixture was diluted with ethyl acetate (100 mL), washed with dilute hydrochloric acid (3 x 40 mL), aqueous sodium bicarbonate (3 x 40 mL) and brine (40 mL). The organic layer was dried (MgSO<sub>4</sub>), filtered and evaporated at reduced pressure to yield 450 mg (55%). <sup>1</sup>H NMR δ 4.8 (s, 2H), 7.4 (m, 2H), 7.6 (d, 2H, *J* = 9.0 Hz), 7.7 (s,

H), 7.8 (d, 2H,  $J = 9.0$  Hz), 8.2 (d, H,  $J = 4.8$  Hz), 8.4 (d, H,  $J = 2.4$  Hz), 10.4 (s, H), 12.5 (br, H). Anal. calc. for  $C_{17}H_{13}N_3O_4S$  : C, 57.46; H, 3.69; N, 11.82; Found : C, 57.20; H, 3.67; N, 11.69.

**c. Synthesis of Type-II Compounds:**

5-(3-Trifluoromethyl-phenyl)-furan-2-carboxylic acid [4-(2,4-dioxo-thiazolidin-5-ylidenemethyl)-phenyl]-amide, B:

Compound **B** was synthesized in the same manner as **D** with a mixture of **4** (1.0 g, 4.6 mmol), 5-(3-Trifluoromethyl-phenyl)-furan-2-carboxylic acid or **7** (1.2 g, 4.6 mmol), HOBt (675 mg, 5.06 mmol) and DEC ( 1.0 g, 5.5 mmol), to yield 1.11 g (53%).  $^1H$  NMR  $\delta$  6.9 (d, H), 7.4 (d, H), 7.8 (m, 9H), 9.8 (br, H). Anal. calc. for  $C_{22}H_{13}F_3N_2O_4S$  : C, 57.64; H, 2.86; N, 6.11; Found : C, 57.64; H, 2.83; N, 5.99.

3-p-Tolyl-isoxazole-5-carboxylic acid [4-(2,4-dioxo-thiazolidin-5-ylidenemethyl)-phenyl]-amide, C:

Compound **C** was prepared by using same sequence as **D** with a mixture of **4** (1.0 g, 4.6 mmol), 3-p-Tolyl-isoxazole-5-carboxylic acid, **8** (924 mg, 4.6 mmol), HOBt (675 mg, 5.06 mmol) and DEC ( 1.0 g, 5.5 mmol,) to yield 1.024 g (55%).  $^1H$  NMR  $\delta$  2.4 (s, 3H), 7.4 (d, 2H,  $J = 7.5$  Hz), 7.4 (s, H), 7.6 (d, 2H,  $J = 7.8$  Hz), 7.7 (s, H), 7.8 (d, 2H,  $J = 7.9$  Hz), 7.9 (d, 2H,  $J = 7.9$ Hz). Anal. calc. for  $C_{21}H_{15}N_3O_4S$  : C, 62.21; H, 3.73; N, 10.36; Found : C, 62.42; H, 3.66; N, 10.19.

5-p-Tolyl-furan-2-carboxylic acid [4-(2, 4-dioxo-thiazolidin-5-ylidenemethyl)-phenyl]-amide, F:

Compound **F** was prepared by using same sequence as **B** with a mixture of **4** (1.0 g, 4.6 mmol), 5-[4-Methoxyphenyl]-2-furoic acid, **9** (990 mg, 4.6 mmol), HOBT (675 mg, 5.06 mmol) and DEC ( 1.0 g, 5.5 mmol,) to yield 1.06 g (57%). <sup>1</sup>H NMR δ 2.4 (s, 3H), 7.1 (d, H, *J* = 3.3 Hz), 7.3 (d, 2H, *J* = 8.4 Hz), 7.5 (d, H, *J* = 3.6 Hz), 7.6 (d, 2H, *J* = 9.0 Hz), 7.7 (s, H), 7.9 (d, 2H, 8.4 Hz), 8.0 (d, 2H, *J* = 9.0 Hz), 10.4 (s, H). Anal. calc. for C<sub>22</sub>H<sub>16</sub>N<sub>2</sub>O<sub>4</sub>S·0.25 H<sub>2</sub>O : C, 65.33; H, 3.99; N, 6.93; Found : C, 64.61; H, 4.07; N, 6.85.

#### **4. Functional Studies to Determine the Binding Affinity of PPAR-γ Receptor Modulators.**

To determine, whether the synthesized compounds are capable of binding to PPAR-γ LBD and their binding affinity, we performed functional studies by using a fluorescence-based competitive binding experiment.

##### **A. Assay Mechanism:**

A fluorescence-based competitive binding assay is used to determine relative affinity of the test compounds for the PPAR-γ LBD as shown in Figure 9. This is a technique specially applied to study molecular interactions. In this assay, PPAR-γ LBD is added to Fluormone™ PPAR-γ Green to form a PPAR-γ LBD/Fluormone™ PPAR-γ Green complex.

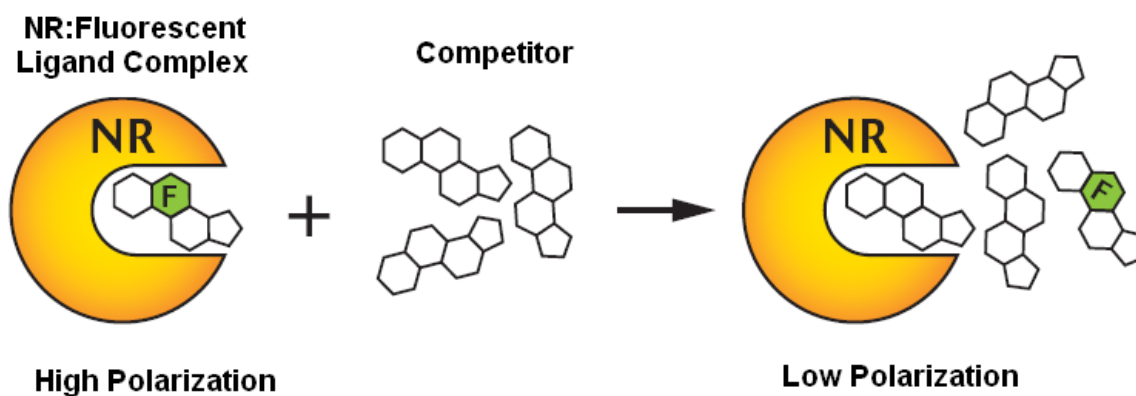


**Figure 9.** Fluorescence based affinity binding assay. NR: nuclear receptor and F is fluorescent ligand.

The binding of PPAR- $\gamma$  LBD to the Fluormone ligand results in high polarization value. This complex is then added to individual test compounds in microwell plates. Competitors or test compounds displace the Fluormone ligand from the PPAR- $\gamma$ -LBD/Fluormone complex, causing the Fluormone ligand to tumble rapidly during its fluorescent lifetime, resulting in a low polarization value. Non-competitors will not displace the Fluormone ligand from the complex, so the polarization value remains high. The shift in polarization value in the presence of test compounds is used to determine the relative affinity of test compounds for PPAR- $\gamma$  LBD.

#### **B. Assay Procedure:**

The PPAR- $\gamma$  LBD receptor binding assay kits (Panvera, Madison, WI) were used to determine the ability of the test molecules to displace the fluormone, PPAR Green, from PPAR- $\gamma$  LBD/ fluormone PPAR Green complex. Serial dilutions of each test molecule were prepared in DMSO. The recombinant PPAR- $\gamma$  LBD (1.1 pM) was pre-incubated with

PPAR Green (2.5 nM) in screening buffer. After the pre-incubation, the test and PPAR- $\gamma$  LBD/ Fluormone ligand complex solution were added into 384-well plate to produce a final volume of 40  $\mu$ L per well. The reaction was incubated at room temperature for 2 hrs and polarization values were measured by using fluorescence microplate reader, Polarion (Tecan Research, Triangle Park, NC) with excitation wavelength 495 nm and emission wavelength 535 nm. Fluorescent polarization is measured in mP, a polarization unit. The formation of PPAR- $\gamma$  LBD/ Fluormone ligand complex results in highest mP value and is considered as 0 % inhibition value. Hence mP value and % inhibition value are inversely proportional to each other. Addition of ligand to PPAR- $\gamma$  LBD/ Fluormone ligand complex results in lower mP value and higher % inhibition values. The polarization value versus test compound concentration curves was analyzed by Sigma Plot software to generate IC-50 values.

For the intensities, the actual polarization values P (in mP values) were calculated by using the following formula:

$$P = \frac{I_{\parallel} - I_{\perp}}{I_{\parallel} + I_{\perp}}$$

Where P is polarization unit, we measure polarization in mP values.

$I_{\parallel}$  = intensity parallel.

$I_{\perp}$  = intensity perpendicular.



5. **Structural studies of PPAR- $\gamma$  LBD in complex with PPAR- $\gamma$  receptor modulators.**

X-ray crystallography was used to elucidate the binding modes of these synthesized compounds to PPAR- $\gamma$  LBD. Hanging drop vapor diffusion method (shown in Figure 10) was used for the crystallization experiments. In the experiment, a droplet of purified protein, buffer and precipitant is allowed to equilibrate with a larger reservoir containing similar buffer and precipitant in higher concentrations.

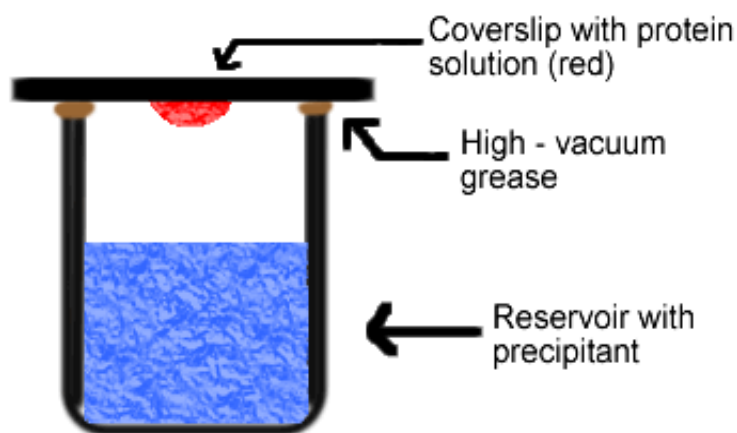


**Figure 10.** Protein crystallization: Hanging drop vapor diffusion method. Reservoir solution (blue) usually contains buffer and precipitant. Protein solution (red) contains the same compounds, but in lower concentrations. The protein solution may also contain trace metals or ions necessary for precipitation of particular proteins.<sup>88</sup>

**A. Crystallization of Complex**

Crystallization of PPAR- $\gamma$  LBD with various active compounds was carried out using excess of the ligand. Rosiglitazone, compound **A** and **B** were dissolved in dimethyl

sulfoxide (DMSO), and were added to the protein (15 mg/mL) solution at a 10:1 molar excess to encourage complete binding, and then incubated on ice for 1 hour prior to crystallization trials. Initial crystallization trials for the His-tagged PPAR- $\gamma$  LBD in complex with the ligands were conducted using the Crystal screening kit I and II (Hampton Research) at 4°C, 15°C and room temperature (25°C). We obtained micro-crystals in previously established crystal conditions as shown below.<sup>62, 89, 90</sup>

1.4 M Sodium Citrate (pH 5.6), 100 mM HEPES (pH 7.5).

1. 1.4 M Sodium Citrate (pH 5.6), 20 mM tris HCl (pH 8.0).

2. 4.0 M Sodium Formate.

Following, we optimized these conditions to obtain X-ray quality crystals. First, we optimized the condition 1 above. The crystallization drop was set up using protein (15 mg/ml in 50mM NaCl, 25 mM Tris-HCl, pH 8.0, 5mM DTT), and a reservoir solution of 1.0 - 1.5 M Sodium Citrate (pH 5.6), 100 mM HEPES (pH 7.5).

The crystallization condition 2 was also optimized by setting up crystal drop with varying reservoir solution concentrations from 0.8 M – 1.6 M Sodium Citrate (pH 5.6), 20 mM tris HCl (pH 8.0), at 4° C and also at 20°C. The protein concentration was also varied. The 3<sup>rd</sup> crystallization condition which showed the most encouraging results was also modified. The crystal drop contains 10 mg/ml protein concentration with reservoir solution consisting of PEG 20,000 (10% - 30%), 0.1 M MES, at 4°C and 15°C.

## **{CHAPTER III Results and Discussion}**

### **1. Expression and Purification of PPAR- $\gamma$ LBD.**

The protein was first expressed and purified as the Glutathione S Transferase-tagged (GST-tagged) fusion protein in order to aid in purification. GST was originally selected as a fusion moiety because of several desirable properties. First and foremost, when expressed in bacteria alone, or in fusion, GST is not sequestered in inclusion bodies. Second, GST can be affinity purified without denaturation because it binds to immobilized glutathione, which provides the basis for simple purification.

To make the recombinant protein, the pGEX-4T1 vector with fused GST was expressed in *E. coli* Rosetta (DE3) cells. The protein was precipitated using ammonium sulfate precipitations (up to 65%). Ammonium sulfate precipitated only PPAR- $\gamma$ , which ensured the elimination of intrinsic *E. coli* PK from the protein mixture. The precipitated fraction was dissolved in 1 X PBS, pH 7.4 and 1 mM DTT containing 1 mM phenylmethylsulfonyl fluoride and also dialyzed overnight against the same buffer. The dialyzed protein was then loaded onto the previously equilibrated GST-column with 1 X PBS for purification. After washing with the 2 column volume 1 X PBS, the GST moiety was removed by digesting the fusion protein with the help of thrombin (Pharmacia) on the column. Then the cleaved

PPAR- $\gamma$  LBD was eluted with the help of elution buffer. The results of PPAR- $\gamma$  expression and purification are shown in Table 2. The protein yield was 5mg/L determined using Bradford assay. The purified enzyme also showed activity in the subsequent PPAR- $\gamma$  LBD fluorescent assay. SDS PAGE gel in Figure 11 showed a good protein expression, however the purified protein still contained contaminants. Subsequently, the impure fraction was further purified using SEPHADEX 200 column, which did not help to separate the impure fraction from the pure protein fraction. Thus, the use of GST for making the protein was not very successful, as the quantities and purity of the PPAR- $\gamma$  LBD obtained at 32 KDa were minimal. The process was also cumbersome and expensive.

To overcome this, we decided to use a different vector, pET28a (+) with His-tag and an alternate method of purification. First, the PPAR- $\gamma$  LBD cloned in pET28a (+) plasmid (Novagen) was obtained from our Brazilian collaborators, Dr. Polikarpov and colleagues, and transferred to competent Rossetta cells (Strat-agene). The attached N-terminal His-tag allowed PPAR- $\gamma$  LBD's to be purified by a single step Ni-NTA column chromatography. Using this approach, the yield of pure PPAR- $\gamma$  LBD improved significantly up to 3-fold, typically 15 mg/L. Figure 12 shows the SDS- PAGE gel of the purified enzyme. Thus expression of the protein in Rosetta cells with the attached His-tag represents a new simple method providing improved yield for the expression and purification of PPAR- $\gamma$  LBD.

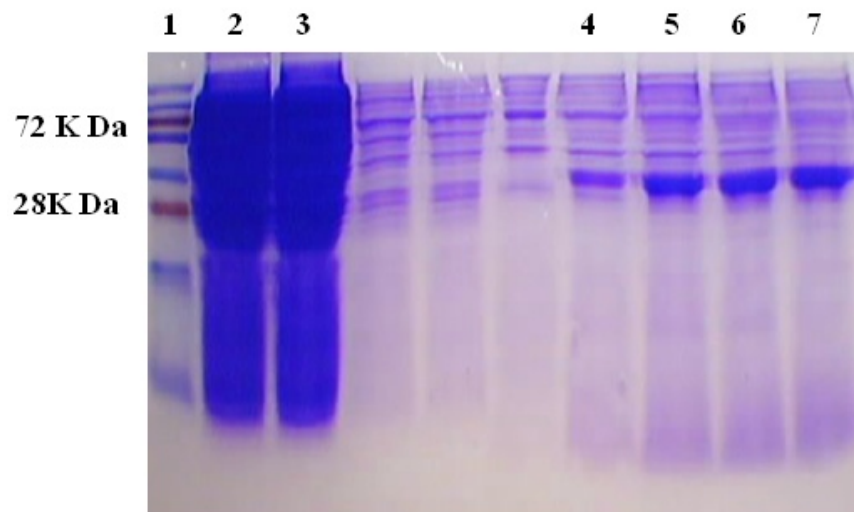


**Figure 11.** 10% SDS-PAGE gel of PPAR- $\gamma$  LBD protein purified using the procedure recommended by manufacturer (Amersham Pharmacia Biotech). Three fractions of protein were run in parallel with molecular mass standards. Lanes (1) Protein standard (Fermentas), (2) After cell brake GST- bound PPAR- $\gamma$  LBD, (3) After ammonium sulfate GST- bound PPAR- $\gamma$  LBD, (4) protein elution PPAR- $\gamma$  LBD 1, (5), (6) and (7) are protein elutions 2, 3 and 4 respectively.

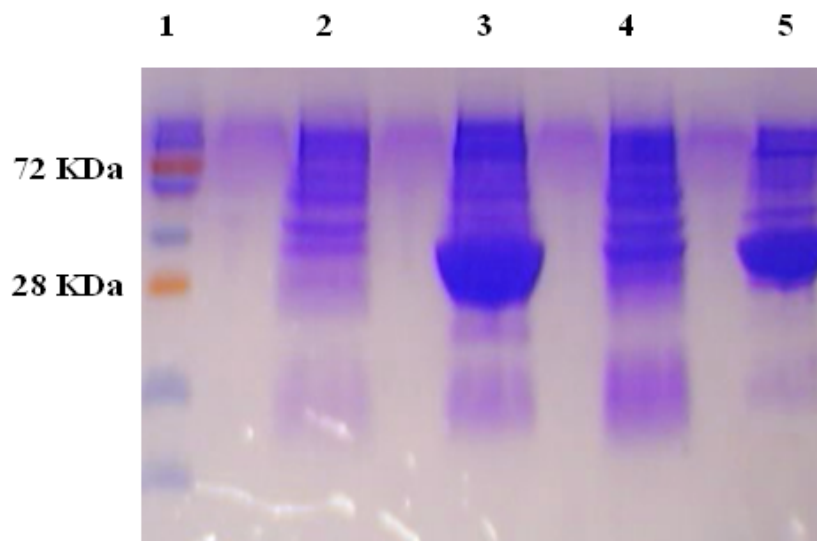


**Figure 12.** 10% SDS-PAGE gel of PPAR- $\gamma$  LBD purified protein. Lanes (1) Protein standard (Fermentas), (2) and (4) are washing, (3) and (5) show varying concentrations of PPAR- $\gamma$  LBD with attached His tag.

**Table 2.** Yield of PPAR- $\gamma$  LBD protein with two different expression vectors.

Method	Yield (mg/L)
pGEX-4T1 + GST	5
pET 28a (+) + His-tag	15

## **2. Molecular Modeling to Design PPAR- $\gamma$ Receptor Modulators.**

Our aim was to use the structural features and binding mode of Rosiglitazone as a starting point to design novel PPAR- $\gamma$  agonists. A visual analysis of the binding of Rosiglitazone suggests two possible structural modifications; first to the ether linkage and second to the hydrophobic side chain. This culminated into two possible classes of compounds, type-I and type-II compounds. Using SYBYL 7.3, representative molecules of these two classes (compound **A** from type-I and **B** from type-II) were built and energy minimized. These compounds were manually docked into PPAR- $\gamma$  LBD (PDB code 2PRG) using TOM and/or COOT. Minimization of the protein residues around the docked compounds using SYBYL 7.3 yielded several binding orientations. Unexpectedly, none of the binding orientations with high HINT scores corresponded to the crystallographically bound Rosiglitazone's orientation. As a control, we also energy minimized the crystallographically bound Rosiglitazone (Figure 13) using SYBYL 7.3, and also unexpectedly the best binding orientation was not consistent with the crystallographically bound orientation. Based on this, we decided to use the manually fit putative compounds

based on Rosiglitazone binding for design purpose. Figure 14-17 show hypothetical binding of our designed type-I and type-II compounds to the PPAR- $\gamma$  LBD.

As shown in Figure 14 and 15, the thiazolidinedione rings of both compound **A** and Rosiglitazone occupy similar position. Like Rosiglitazone the two oxygen atoms of thiazolidinedione ring of compound **A** are capable of making hydrogen-bond interactions with His323 and His449. Secondly, the newly introduced carbonyl oxygen of the amide linkage in compound **A** is capable of making additional hydrogen-bond interaction with Cys285. Thirdly, the hydrophobic chain was positioned in PPAR- $\gamma$  LBD binding pocket in the same manner as Rosiglitazone.

In the type-II compounds, in addition to the described interactions observed for Rosiglitazone, the amide oxygen can also make hydrogen-bond interaction with Cys285. Also, the increased length of the hydrophobic side chain could make hydrophobic interactions with Ile281, Met348, Ile341 and Arg288. Our hypothesis is that the type-I and -II compounds will have higher affinity to the PPAR- $\gamma$  LBD because of the additional hydrogen-bond and/or hydrophobic interactions with the protein.

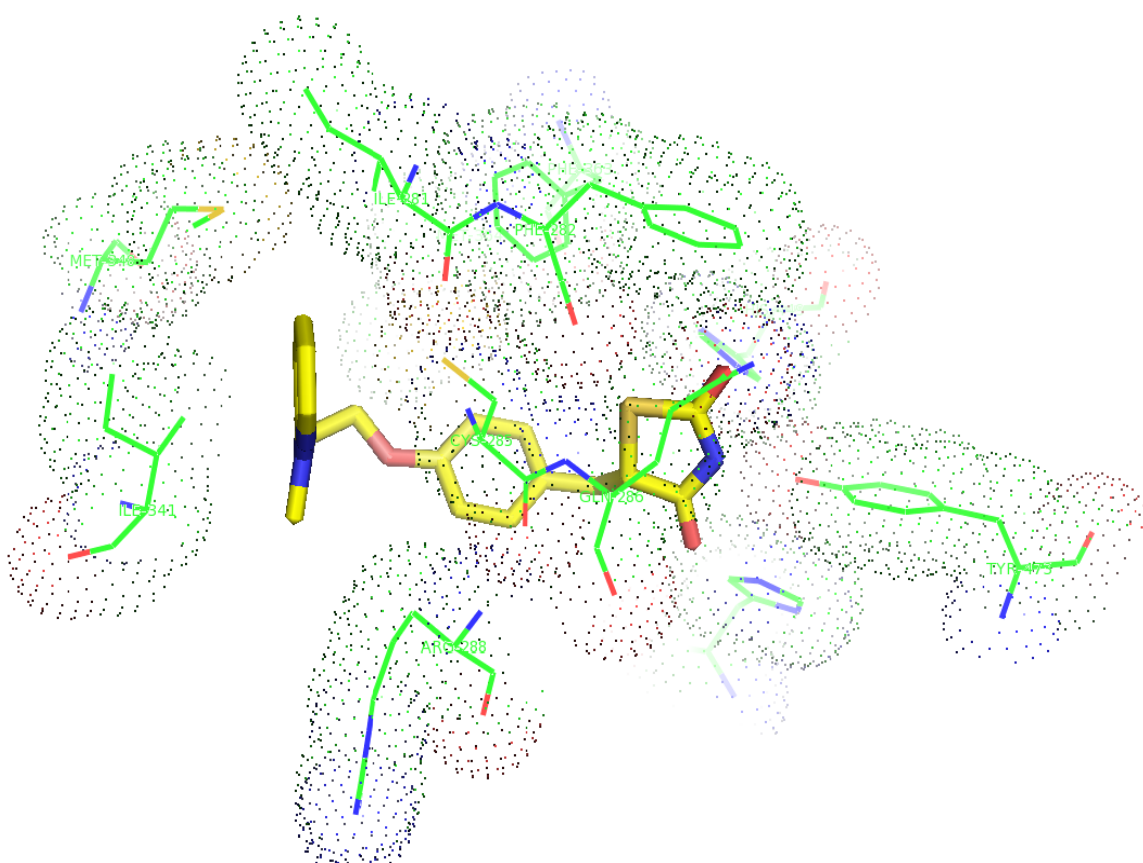


**Figure 13.** Rosiglitazone in crystal structure with PPAR- $\gamma$  LBD.



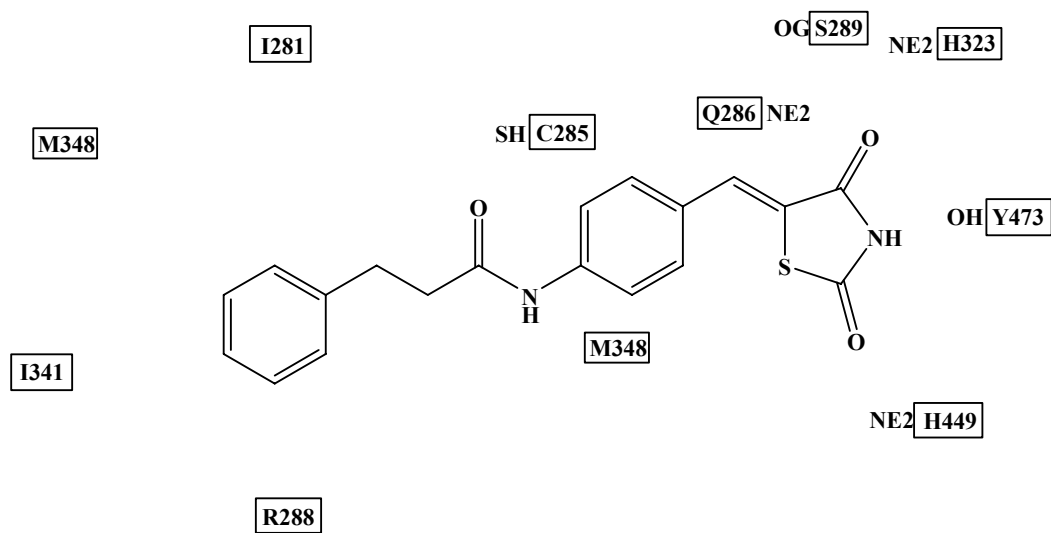


**Figure 14.** Proposed binding mode of Compound A (type-I compound) docked manually in PPAR- $\gamma$  LBD.

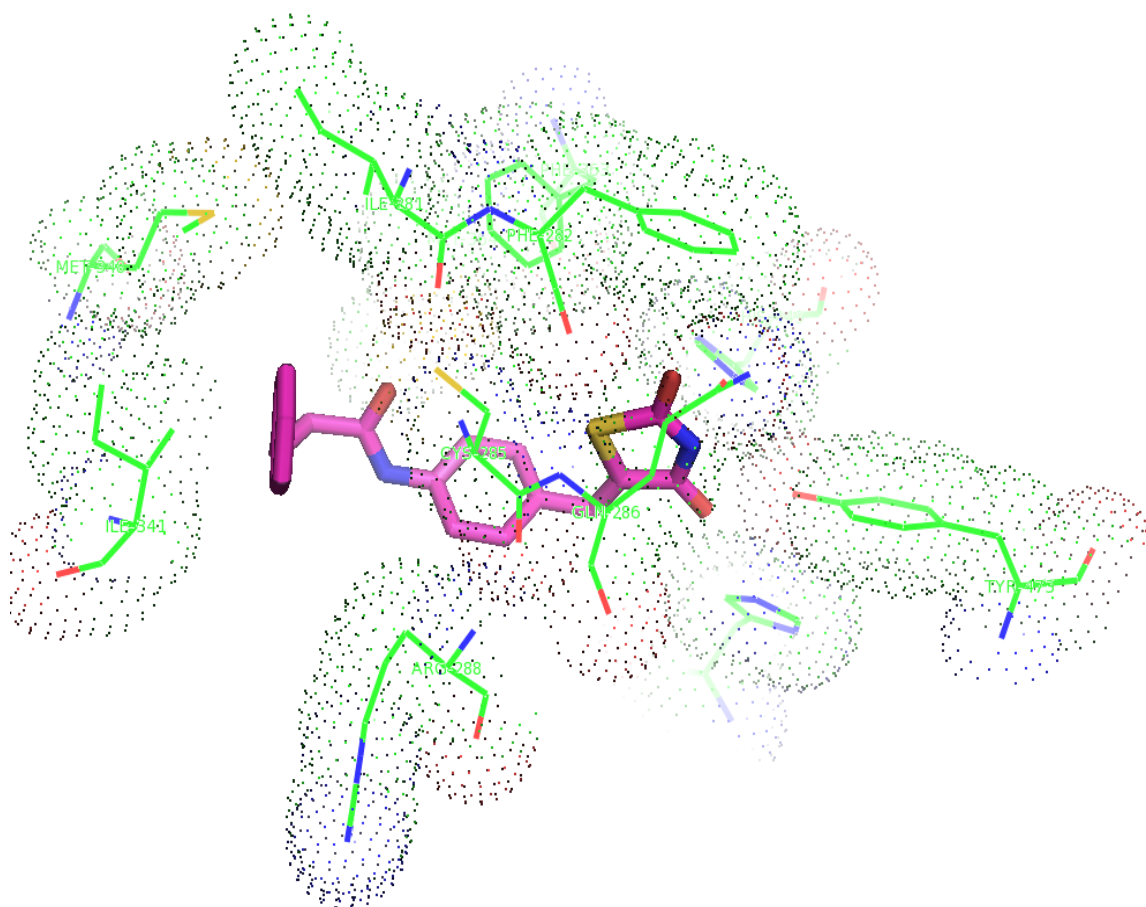


**Figure 15.** Proposed binding mode of compound A (type-I compound) in the PPAR- $\gamma$  LBD complex.

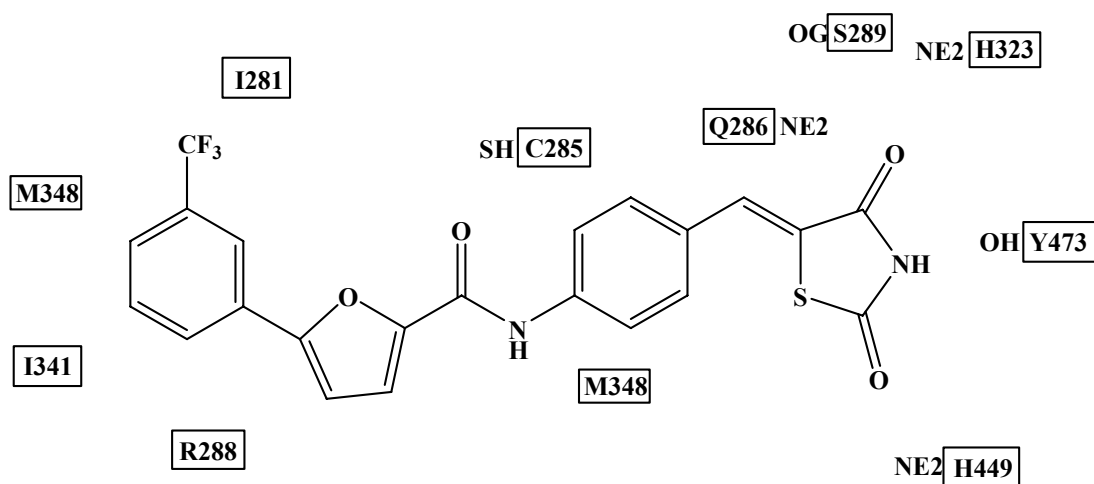


**Figure 16.** Proposed binding mode of compound **B** (type-II compound) docked manually in PPAR- $\gamma$  LBD.

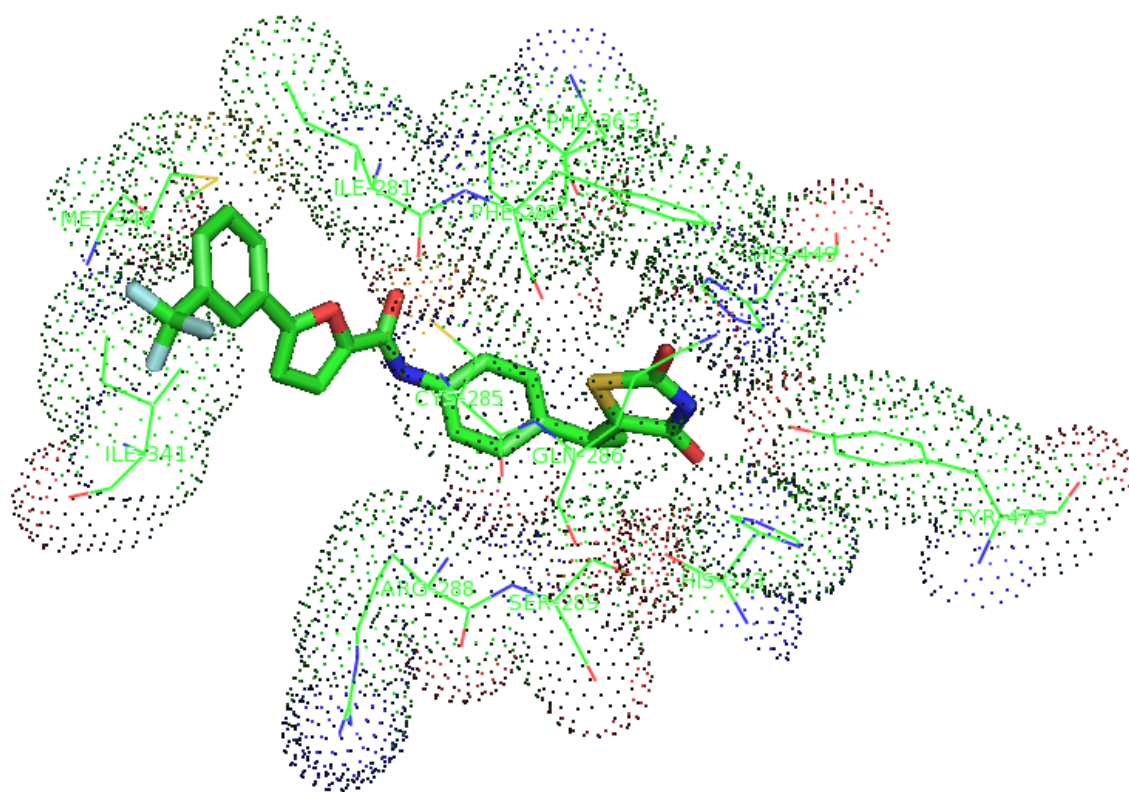


Figure 17. Proposed binding mode of compound **B** (type-II compound) in the PPAR- $\gamma$  LBD complex.

### 3. Synthesis of Potential PPAR- $\gamma$ Receptor Modulators.

The whole synthesis was divided into three schemes. In scheme 1 we synthesized **4**, which would serve as precursor to scheme 2 and 3 for synthesis of both classes of compounds.

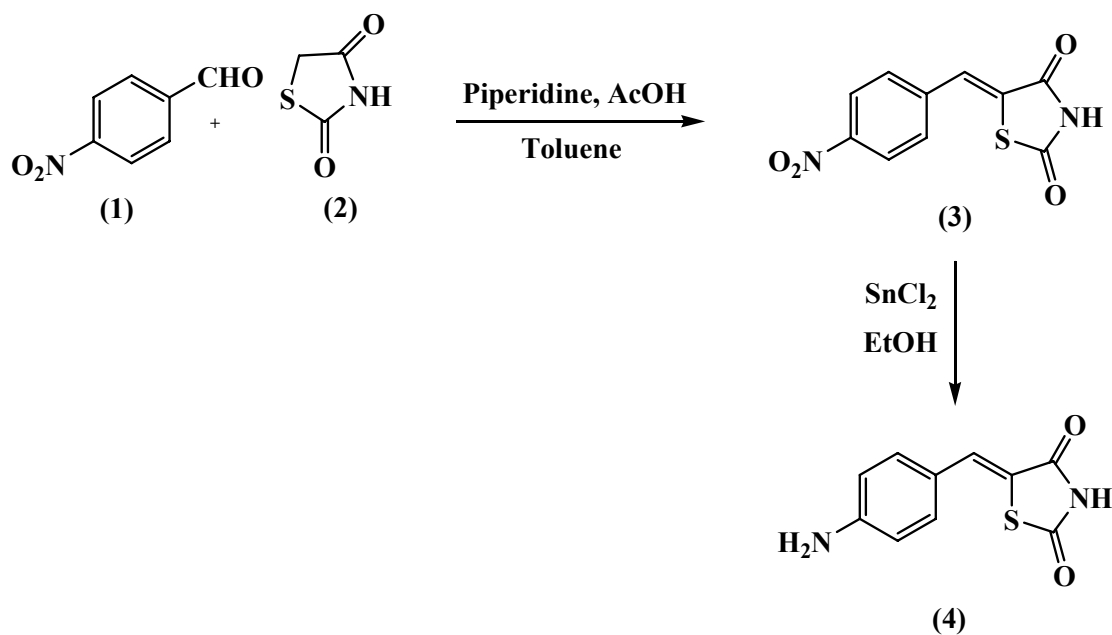
#### A. Intermediates

For synthesis of **4**, a two step approach was adopted, first by mixing the commercially available starting core compound, **1** and **2**, in the presence of piperidine and acetic acid in toluene under stirring condition, for 16-18 hrs at room temperature, **3**, was obtained. In the second step of scheme 1, we reduced the nitro compound to amine. To a stirring solution of **3** in ethanol, we added tin (II) chloride and the mixture heated to reflux for 2-3 hours, to obtain **4**.

#### B. Synthesis of type-I compounds:

In scheme 2, the type-I compounds were synthesized by using **4** as one of the two reactants. Synthesis of five type-I compounds were attempted using two different approaches, however we were only successful in synthesizing two of the compounds, including **A** and **D**. For synthesis of compound **A**, to a mixture of **4** and triethylamine in dichloromethane at 0° C, in presence of nitrogen, hydrocinnamoyl chloride or **5** was added dropwise.

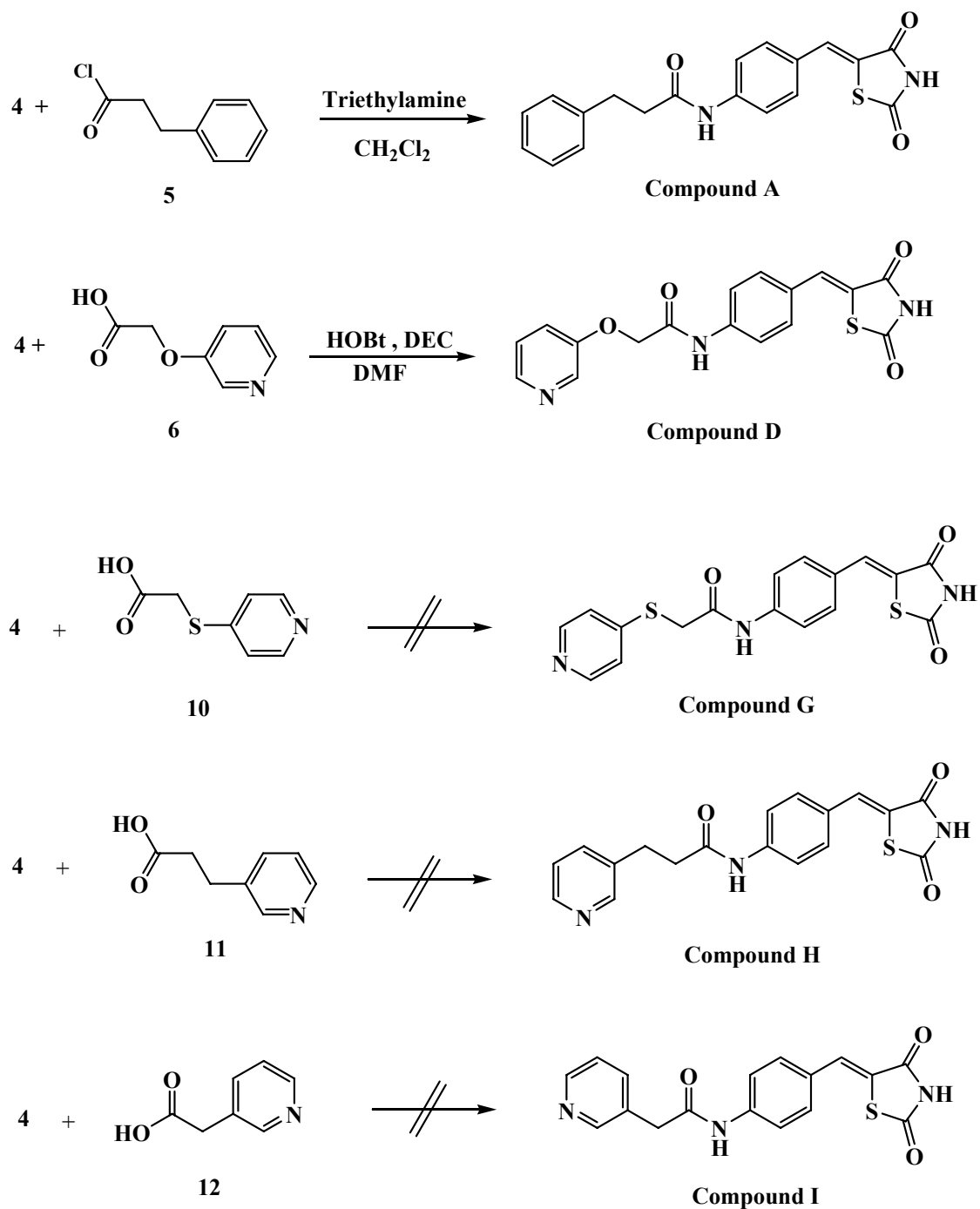
**Scheme 1:**



After stirring at the same temperature for ten minutes, the mixture was further stirred at room temperature for 2 hr, to obtain compound **A**. To a mixture of **4** and **6**, in DMF, in presence of nitrogen at room temperature, HOBt and DEC, were added and the mixture stirred overnight, to obtain compound **D**.

Along with above synthesized compounds shown in scheme 2, synthesis of three more type-I compounds **G**, **H**, **I**, was tried, shown in scheme 2. A similar sequence to that described in scheme 2 for the synthesis of type-I compound **D** was followed. Although TLC showed formation of a new entity, NMR analyses for these three compounds were not consistent with the structures shown below.

**Scheme 2:**



### C. Synthesis of type-II compounds:

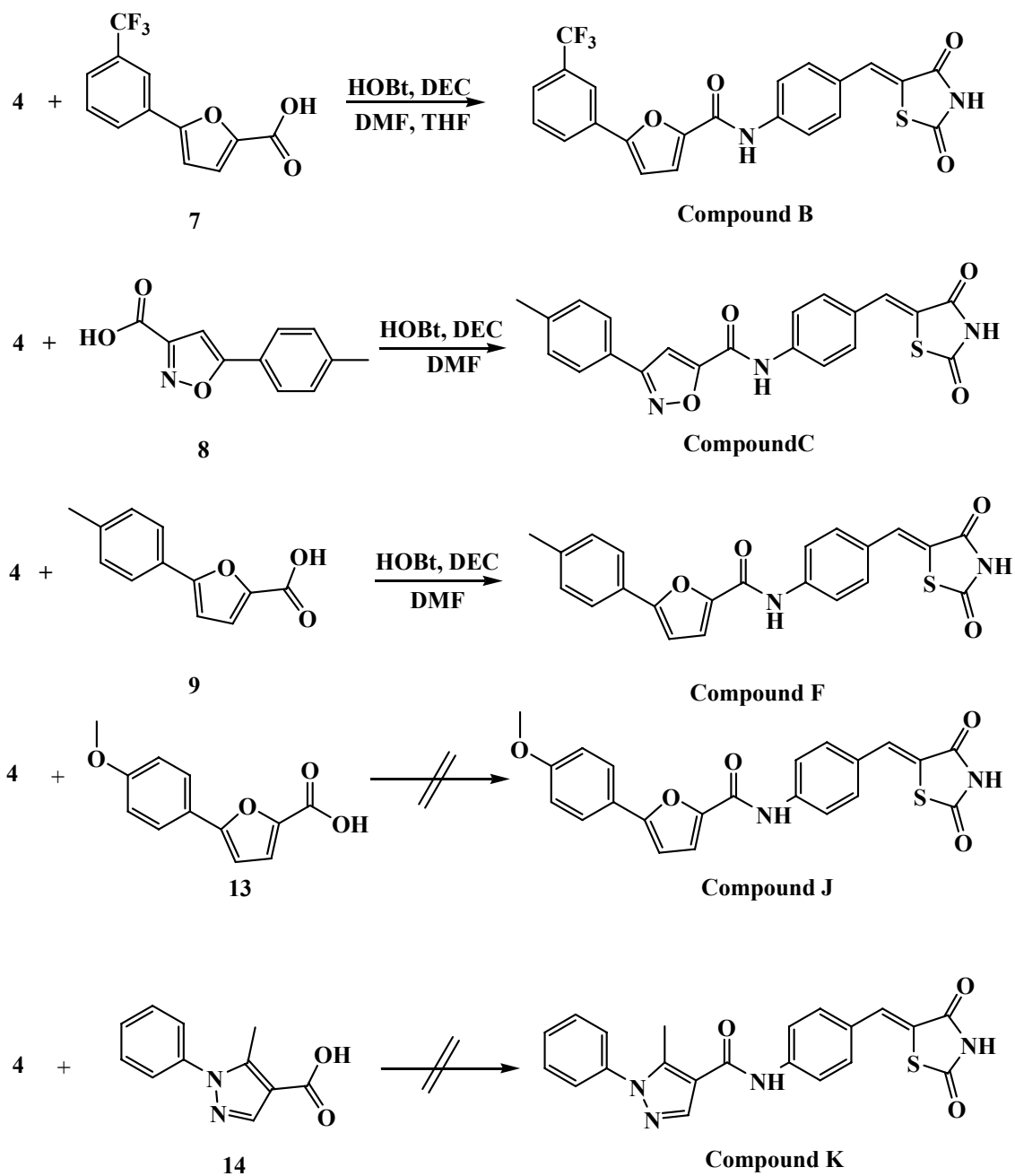
Synthesis of type-II compounds as shown in scheme 3 followed similar sequence as described in scheme 2 for the synthesis of type-I compound **D**. For synthesis of **B**, DMF and THF was added to a mixture of **4** and **7**, under nitrogen at room temperature, along with HOBt and DEC and stirred overnight. For synthesis of **C** and **F** same reaction sequence was followed as shown in scheme 3.

We also carried out the synthesis of two other type-II compounds **J** and **K** by following similar sequence we used in synthesis of **B**, but was unsuccessful as shown in scheme 3. The reaction product precipitated out, and the crude material was not soluble in any solvent.

In conclusion, we have been able to synthesize five compounds, **A**, **B**, **C**, **D** and **F** out of ten that we designed. Synthesis of the other five compounds, **G**, **H**, **I**, **J** and **K** are planned in future using alternate synthetic schemes.



**Scheme 3:**



#### **4. Functional Studies to Determine the Binding Affinity of PPAR- $\gamma$ Receptor Modulators.**

Fluorescent-based competitive binding assay was used to find out whether the synthesized compounds bind to PPAR- $\gamma$  LBD, as well as their binding affinities. Parallel experiments with Rosiglitazone and Troglitazone in our lab were also performed. If tested compound binds to PPAR- $\gamma$  LBD, it should competitively displace the Fluormone ligand from the PPAR- $\gamma$ -LBD/Fluormone ligand complex resulting in a low polarization value. Non-competitors will not displace the Fluormone ligand from the complex, so the polarization value remains high. The shift in polarization value in the presence of test compounds is used to determine relative affinity of the test compounds for the PPAR- $\gamma$  LBD.

Table 3 shows the competitive inhibition of the Fluormone ligand by Rosiglitazone, Troglitazone, compounds **A**, **B**, **C**, **D**, and **F**. Type-I compounds, **A** and **D** shows 74% and 54% inhibition respectively, as compared to 89 and 99% for Rosiglitazone and Troglitazone, respectively. Compound **A** has IC-50 value of 344  $\mu$ M, which translates to a ~1900-fold lower affinity compared to Rosiglitazone (IC-50 value 0.178  $\mu$ M). The IC-50 of compound **D** was not determined but we expect to behave similarly as **A**. Type-II compounds, **B**, **C** and **F** show 98%, 73% and 78% inhibition respectively as compared to 89% of Rosiglitazone. Compound **B** shows a significant binding affinity to PPAR- $\gamma$  LBD, as evidenced by an IC-50 value of 1.3  $\mu$ M, which is ~ 7-fold lower than Rosiglitazone. The IC-50s for the rest of the other compounds were not determined, however based on the % inhibition we speculate that none of them would exhibit higher potency than compound **B**.

It seems that type-II compounds may be more potent than type-I compounds. Most likely, the extra hydrophobic interactions made by type-II compounds with the residues Ile281, Met348, Ile341 and Arg288 in the PPAR- $\gamma$  LBD increase their binding affinity to LBD compared to the type-I compounds.

**Table 3.** The % inhibition and IC-50 values by using Fluorescent Polarization Assay.

S.N.	Compound	% inhibition*	IC <sub>50</sub> ( $\mu$ M)
1.	Rosiglitazone	89	0.178
2.	Troglitazone	99	—
3.	Compound <b>A</b>	74	344
4.	Compound <b>B</b>	98	1.30
5.	Compound <b>C</b>	73	—
6.	Compound <b>D</b>	54	—
7.	Compound <b>F</b>	78	—
8.	TDD4-73	90	9.85
9.	TDD4-84	32	780

\*Compounds used at 25  $\mu$ M concentration.

Our designed compounds were hypothesized to have higher affinity to PPAR- $\gamma$  LBD than Rosiglitazone due to the proposed additional hydrogen-bond interaction with Cys285 and/or hydrophobic interactions with the protein. However, they still show significantly lower affinity to the protein compared to Rosiglitazone. As shown in Figure 8, there is a double bond between the thiazolidinedione ring and the benzene ring of the core structure of our compounds, which is a single bond in Rosiglitazone. Thus, the thiazolidinedione ring in Rosiglitazone can easily rotate in the binding pocket, which is unlikely with our

compounds. We note that the two hydrogen-bond interactions between the two carbonyl oxygens of thiazolidinedione ring and His323 and His449 are the most important for binding. Therefore, it is most likely that Rosiglitazone with a flexible thiazolidinedione ring can easily bind to make optimal interactions with both His323 and His449. This is unlikely in our compounds, where the ring is rigid and fixed at one orientation. We are currently synthesizing analogs of our compounds with a single bond between the ring and the benzene. Our hypothesis is that these compounds will result in better binding affinity.

## **5. Structural Studies of PPAR- $\gamma$ LBD in Complex with PPAR- $\gamma$ Receptor Modulators.**

Structure-based drug design is one of the most logical approaches applied in drug discovery. It integrates information from several fields, such as X-ray crystallography, molecular modeling, synthetic organic chemistry, quantitative structure-activity relationship (QSAR) studies, and biological evaluation to identify new lead molecules that can interact specifically with the target protein structure. This is a cyclic procedure that refines each stage of discovery. This structural information obtained from X-ray crystallography enables design of new molecules or ligands, and eventually drugs that interfere with the binding of natural ligands to the proteins and consequently alter their biological function.<sup>91</sup>

X-ray crystallographic study was thus attempted in order to determine the binding mode of our compounds with the PPAR- $\gamma$  LBD. Crystallization experiments were conducted in the absence and presence of Rosiglitazone, type-I and -II compounds. Initially crystallization

conditions for the His-tagged PPAR- $\gamma$  LBD complex, were tried using the crystal screening kit I and II (Hampton Research) at 20°C. Several crystallization conditions were then optimized further by fine gridding around the initial conditions. Also, previously published crystallization conditions were used for crystallizing the complex. None of these experiments yielded X-ray quality crystals, and thus we have been unable to determine the co-crystal structures of these compounds with PPAR- $\gamma$  LBD.

### **{CHAPTER 3 Summary and Conclusion}**

At present, there are two marketed TZDs, Rosiglitazone and Pioglitazone, currently being used as first line treatment of type-II diabetes. There has been report of serious side effect for Rosiglitazone. A review of the studies of Rosiglitazone led the FDA to conclude that the medication might increase the risk of heart attacks and angina, but it's not clear what the cause is, but there are speculations that this could be due to Rosiglitazone metabolites. The drug is still being used but with a BOXED warning.

The development of new type-II diabetes drug that work similarly as Rosiglitazone but with less side effect and possibly with increased potency is much needed and very urgent. The main goal of the study is to develop a potential TZD agonist with improved activity and minimal side effects. In this study, PPAR- $\gamma$  LBD was purified with simple and efficient method and also resulted in significant yield. Molecular modeling studies helped in identification of potential PPAR- $\gamma$  agonists, which were synthesized. These compounds were designed to make additional hydrogen-bond and/or hydrophobic interaction with the protein. Our hypothesis is that these additional binding will lead to increase affinity and perhaps better agonist. For the type-I compounds, containing thiazolidinedione ring and carbonyl oxygen of the amide bond, their binding affinity were found to be significantly lower than Rosiglitazone. Type-II compounds have additional hydrophobic ring attached

with different functional group on it. The binding affinity of these compounds is relatively higher and better than type-I compounds but still significantly lower than Rosiglitazone. This unexpected difference in binding affinity between Rosiglitazone and both type-I and type-II compounds is most probably due to the fact that thiazolidinedione ring in Rosiglitazone can easily rotate to make optimal interactions with the protein residues His323 and His449, which are known to be very important for binding affinity and agonistic activity. This is not the case in our compounds where the double bond between the thiazolidinedione ring and the benzene makes the thiazolidinedione ring unable to rotate and perhaps make optimal contact with the residues His323 and His449. Our collaborators from The Scripps Research Institute (Scripps Florida) are currently testing our compounds for their agonistic activity. We are also synthesizing analogs of these compounds with flexible thiazolidinedione ring system. To find out the important interactions between PPAR- $\gamma$  LBD and synthesized compounds, crystallization studies were attempted but failed. Crystallization attempts are ongoing in order to solve the PPAR- $\gamma$  LBD structure in complex with our ligands.

### **Literature Cited**

1. Evans, R. M. The steroid and thyroid hormone receptor superfamily. *Science* **1988**, 240, 889-95.
2. Olefsky, J. M. Nuclear receptor minireview series. *J Biol Chem* **2001**, 276, 36863-4.
3. Novac, N.; Heinzl, T. Nuclear receptors: overview and classification. *Curr Drug Targets Inflamm Allergy* **2004**, 3, 335-46.
4. Mangelsdorf, D. J.; Thummel, C.; Beato, M.; Herrlich, P.; Schutz, G.; Umesono, K.; Blumberg, B.; Kastner, P.; Mark, M.; Chambon, P.; Evans, R. M. The nuclear receptor superfamily: the second decade. *Cell* **1995**, 83, 835-9.
5. Di Croce, L.; Okret, S.; Kersten, S.; Gustafsson, J. A.; Parker, M.; Wahli, W.; Beato, M. Steroid and nuclear receptors. Villefranche-sur-Mer, France, May 25-27, 1999. *EMBO J* **1999**, 18, 6201-10.
6. Evans, R. A transcriptional basis for physiology. *Nat Med* **2004**, 10, 1022-6.
7. Maglich, J. M.; Sluder, A.; Guan, X.; Shi, Y.; McKee, D. D.; Carrick, K.; Kamdar, K.; Willson, T. M.; Moore, J. T. Comparison of complete nuclear receptor sets from the human, *Caenorhabditis elegans* and *Drosophila* genomes. *Genome Biol* **2001**, 2, RESEARCH0029.



8. Sonoda, J.; Pei, L.; Evans, R. M. Nuclear receptors: decoding metabolic disease. *FEBS Lett* **2008**, 582, 2-9.
9. Szanto, A.; Narkar, V.; Shen, Q.; Uray, I. P.; Davies, P. J.; Nagy, L. Retinoid X receptors: X-ploring their (patho)physiological functions. *Cell Death Differ* **2004**, 11 Suppl 2, S126-43.
10. Shulman, A. I.; Mangelsdorf, D. J. Retinoid x receptor heterodimers in the metabolic syndrome. *N Engl J Med* **2005**, 353, 604-15.
11. Li, Y.; Lambert, M. H.; Xu, H. E. Activation of nuclear receptors: a perspective from structural genomics. *Structure* **2003**, 11, 741-6.
12. Levin, E. R. Integration of the extranuclear and nuclear actions of estrogen. *Mol Endocrinol* **2005**, 19, 1951-9.
13. Li, X.; Huang, J.; Yi, P.; Bambara, R. A.; Hilf, R.; Muyan, M. Single-chain estrogen receptors (ERs) reveal that the ERalpha/beta heterodimer emulates functions of the ERalpha dimer in genomic estrogen signaling pathways. *Mol Cell Biol* **2004**, 24, 7681-94.
14. Kansra, S.; Yamagata, S.; Sneade, L.; Foster, L.; Ben-Jonathan, N. Differential effects of estrogen receptor antagonists on pituitary lactotroph proliferation and prolactin release. *Mol Cell Endocrinol* **2005**, 239, 27-36.
15. Shang, Y.; Brown, M. Molecular determinants for the tissue specificity of SERMs. *Science* **2002**, 295, 2465-8.
16. Deroo, B. J.; Korach, K. S. Estrogen receptors and human disease. *J Clin Invest* **2006**, 116, 561-70.

17. Issemann, I.; Green, S. Activation of a member of the steroid hormone receptor superfamily by peroxisome proliferators. *Nature* **1990**, 347, 645-50.
18. Dreyer, C.; Krey, G.; Keller, H.; Givel, F.; Helftenbein, G.; Wahli, W. Control of the peroxisomal beta-oxidation pathway by a novel family of nuclear hormone receptors. *Cell* **1992**, 68, 879-87.
19. Zhu, Y.; Alvares, K.; Huang, Q.; Rao, M. S.; Reddy, J. K. Cloning of a new member of the peroxisome proliferator-activated receptor gene family from mouse liver. *J Biol Chem* **1993**, 268, 26817-20.
20. Greene, M. E.; Blumberg, B.; McBride, O. W.; Yi, H. F.; Kronquist, K.; Kwan, K.; Hsieh, L.; Greene, G.; Nimer, S. D. Isolation of the human peroxisome proliferator activated receptor gamma cDNA: expression in hematopoietic cells and chromosomal mapping. *Gene Expr* **1995**, 4, 281-99.
21. Kliewer, S. A.; Forman, B. M.; Blumberg, B.; Ong, E. S.; Borgmeyer, U.; Mangelsdorf, D. J.; Umesono, K.; Evans, R. M. Differential expression and activation of a family of murine peroxisome proliferator-activated receptors. *Proc Natl Acad Sci U S A* **1994**, 91, 7355-9.
22. Fajas, L.; Fruchart, J. C.; Auwerx, J. PPARgamma3 mRNA: a distinct PPARgamma mRNA subtype transcribed from an independent promoter. *FEBS Lett* **1998**, 438, 55-60.
23. Fajas, L.; Auboeuf, D.; Raspe, E.; Schoonjans, K.; Lefebvre, A. M.; Saladin, R.; Najib, J.; Laville, M.; Fruchart, J. C.; Deeb, S.; Vidal-Puig, A.; Flier, J.; Briggs, M.

- R.; Staels, B.; Vidal, H.; Auwerx, J. The organization, promoter analysis, and expression of the human PPAR $\gamma$  gene. *J Biol Chem* **1997**, 272, 18779-89.
24. Sundvold, H.; Lien, S. Identification of a novel peroxisome proliferator-activated receptor (PPAR)  $\gamma$  promoter in man and transactivation by the nuclear receptor ROR $\alpha$ 1. *Biochem Biophys Res Commun* **2001**, 287, 383-90.
25. Tontonoz, P.; Hu, E.; Spiegelman, B. M. Stimulation of adipogenesis in fibroblasts by PPAR  $\gamma$  2, a lipid-activated transcription factor. *Cell* **1994**, 79, 1147-56.
26. Spiegelman, B. M.; Flier, J. S. Adipogenesis and obesity: rounding out the big picture. *Cell* **1996**, 87, 377-89.
27. Crabtree, G. R. Generic signals and specific outcomes: signaling through Ca<sup>2+</sup>, calcineurin, and NF-AT. *Cell* **1999**, 96, 611-4.
28. Ristow, M.; Muller-Wieland, D.; Pfeiffer, A.; Krone, W.; Kahn, C. R. Obesity associated with a mutation in a genetic regulator of adipocyte differentiation. *N Engl J Med* **1998**, 339, 953-9.
29. Hegele, R. A.; Cao, H.; Frankowski, C.; Mathews, S. T.; Leff, T. PPARG F388L, a transactivation-deficient mutant, in familial partial lipodystrophy. *Diabetes* **2002**, 51, 3586-90.
30. Kliewer, S. A.; Umesono, K.; Noonan, D. J.; Heyman, R. A.; Evans, R. M. Convergence of 9-cis retinoic acid and peroxisome proliferator signalling pathways through heterodimer formation of their receptors. *Nature* **1992**, 358, 771-4.
31. Keller, H.; Dreyer, C.; Medin, J.; Mahfoudi, A.; Ozato, K.; Wahli, W. Fatty acids and retinoids control lipid metabolism through activation of peroxisome

- proliferator-activated receptor-retinoid X receptor heterodimers. *Proc Natl Acad Sci U S A* **1993**, 90, 2160-4.
32. Michalik, L.; Auwerx, J.; Berger, J. P.; Chatterjee, V. K.; Glass, C. K.; Gonzalez, F. J.; Grimaldi, P. A.; Kadowaki, T.; Lazar, M. A.; O'Rahilly, S.; Palmer, C. N.; Plutzky, J.; Reddy, J. K.; Spiegelman, B. M.; Staels, B.; Wahli, W. International Union of Pharmacology. LXI. Peroxisome proliferator-activated receptors. *Pharmacol Rev* **2006**, 58, 726-41.
  33. Guan, H. P.; Ishizuka, T.; Chui, P. C.; Lehrke, M.; Lazar, M. A. Corepressors selectively control the transcriptional activity of PPARgamma in adipocytes. *Genes Dev* **2005**, 19, 453-61.
  34. Yu, C.; Markan, K.; Temple, K. A.; Deplewski, D.; Brady, M. J.; Cohen, R. N. The nuclear receptor corepressors NCoR and SMRT decrease peroxisome proliferator-activated receptor gamma transcriptional activity and repress 3T3-L1 adipogenesis. *J Biol Chem* **2005**, 280, 13600-5.
  35. Owen, G. I.; Zelent, A. Origins and evolutionary diversification of the nuclear receptor superfamily. *Cell Mol Life Sci* **2000**, 57, 809-27.
  36. A, I. J.; Jeannin, E.; Wahli, W.; Desvergne, B. Polarity and specific sequence requirements of peroxisome proliferator-activated receptor (PPAR)/retinoid X receptor heterodimer binding to DNA. A functional analysis of the malic enzyme gene PPAR response element. *J Biol Chem* **1997**, 272, 20108-17.

37. Kliewer, S. A.; Umesono, K.; Mangelsdorf, D. J.; Evans, R. M. Retinoid X receptor interacts with nuclear receptors in retinoic acid, thyroid hormone and vitamin D3 signalling. *Nature* **1992**, 355, 446-9.
38. Puigserver, P.; Wu, Z.; Park, C. W.; Graves, R.; Wright, M.; Spiegelman, B. M. A cold-inducible coactivator of nuclear receptors linked to adaptive thermogenesis. *Cell* **1998**, 92, 829-39.
39. Vega, R. B.; Huss, J. M.; Kelly, D. P. The coactivator PGC-1 cooperates with peroxisome proliferator-activated receptor alpha in transcriptional control of nuclear genes encoding mitochondrial fatty acid oxidation enzymes. *Mol Cell Biol* **2000**, 20, 1868-76.
40. Wang, Y. X.; Lee, C. H.; Tiep, S.; Yu, R. T.; Ham, J.; Kang, H.; Evans, R. M. Peroxisome-proliferator-activated receptor delta activates fat metabolism to prevent obesity. *Cell* **2003**, 113, 159-70.
41. Zieleniak, A.; Wojcik, M.; Wozniak, L. A. Structure and physiological functions of the human peroxisome proliferator-activated receptor gamma. *Arch Immunol Ther Exp (Warsz)* **2008**, 56, 331-45.
42. Lefebvre, P.; Chinetti, G.; Fruchart, J. C.; Staels, B. Sorting out the roles of PPAR alpha in energy metabolism and vascular homeostasis. *J Clin Invest* **2006**, 116, 571-80.
43. Reddy, J. K.; Hashimoto, T. Peroxisomal beta-oxidation and peroxisome proliferator-activated receptor alpha: an adaptive metabolic system. *Annu Rev Nutr* **2001**, 21, 193-230.

44. Kim, H.; Haluzik, M.; Asghar, Z.; Yau, D.; Joseph, J. W.; Fernandez, A. M.; Reitman, M. L.; Yakar, S.; Stannard, B.; Heron-Milhavet, L.; Wheeler, M. B.; LeRoith, D. Peroxisome proliferator-activated receptor-alpha agonist treatment in a transgenic model of type 2 diabetes reverses the lipotoxic state and improves glucose homeostasis. *Diabetes* **2003**, 52, 1770-8.
45. Berger, J. P.; Akiyama, T. E.; Meinke, P. T. PPARs: therapeutic targets for metabolic disease. *Trends Pharmacol Sci* **2005**, 26, 244-51.
46. Nadra, K.; Anghel, S. I.; Joye, E.; Tan, N. S.; Basu-Modak, S.; Trono, D.; Wahli, W.; Desvergne, B. Differentiation of trophoblast giant cells and their metabolic functions are dependent on peroxisome proliferator-activated receptor beta/delta. *Mol Cell Biol* **2006**, 26, 3266-81.
47. Varnat, F.; Heggeler, B. B.; Grisel, P.; Boucard, N.; Cortesy-Theulaz, I.; Wahli, W.; Desvergne, B. PPARbeta/delta regulates paneth cell differentiation via controlling the hedgehog signaling pathway. *Gastroenterology* **2006**, 131, 538-53.
48. Michalik, L.; Wahli, W. Involvement of PPAR nuclear receptors in tissue injury and wound repair. *J Clin Invest* **2006**, 116, 598-606.
49. He, W.; Barak, Y.; Hevener, A.; Olson, P.; Liao, D.; Le, J.; Nelson, M.; Ong, E.; Olefsky, J. M.; Evans, R. M. Adipose-specific peroxisome proliferator-activated receptor gamma knockout causes insulin resistance in fat and liver but not in muscle. *Proc Natl Acad Sci U S A* **2003**, 100, 15712-7.
50. Koutnikova, H.; Cock, T. A.; Watanabe, M.; Houten, S. M.; Champy, M. F.; Dierich, A.; Auwerx, J. Compensation by the muscle limits the metabolic

- consequences of lipodystrophy in PPAR gamma hypomorphic mice. *Proc Natl Acad Sci U S A* **2003**, 100, 14457-62.
51. Savage, D. B.; Tan, G. D.; Acerini, C. L.; Jebb, S. A.; Agostini, M.; Gurnell, M.; Williams, R. L.; Umpleby, A. M.; Thomas, E. L.; Bell, J. D.; Dixon, A. K.; Dunne, F.; Boiani, R.; Cinti, S.; Vidal-Puig, A.; Karpe, F.; Chatterjee, V. K.; O'Rahilly, S. Human metabolic syndrome resulting from dominant-negative mutations in the nuclear receptor peroxisome proliferator-activated receptor-gamma. *Diabetes* **2003**, 52, 910-7.
  52. Ricote, M.; Li, A. C.; Willson, T. M.; Kelly, C. J.; Glass, C. K. The peroxisome proliferator-activated receptor-gamma is a negative regulator of macrophage activation. *Nature* **1998**, 391, 79-82.
  53. Mayerson, A. B.; Hundal, R. S.; Dufour, S.; Lebon, V.; Befroy, D.; Cline, G. W.; Enocksson, S.; Inzucchi, S. E.; Shulman, G. I.; Petersen, K. F. The effects of rosiglitazone on insulin sensitivity, lipolysis, and hepatic and skeletal muscle triglyceride content in patients with type 2 diabetes. *Diabetes* **2002**, 51, 797-802.
  54. Bajaj, M.; Suraamornkul, S.; Pratipanawatr, T.; Hardies, L. J.; Pratipanawatr, W.; Glass, L.; Cersosimo, E.; Miyazaki, Y.; DeFronzo, R. A. Pioglitazone reduces hepatic fat content and augments splanchnic glucose uptake in patients with type 2 diabetes. *Diabetes* **2003**, 52, 1364-70.
  55. Semple, R. K.; Chatterjee, V. K.; O'Rahilly, S. PPAR gamma and human metabolic disease. *J Clin Invest* **2006**, 116, 581-9.

56. Michalik, L.; Desvergne, B.; Wahli, W. Peroxisome-proliferator-activated receptors and cancers: complex stories. *Nat Rev Cancer* **2004**, 4, 61-70.
57. Burdick, A. D.; Kim, D. J.; Peraza, M. A.; Gonzalez, F. J.; Peters, J. M. The role of peroxisome proliferator-activated receptor-beta/delta in epithelial cell growth and differentiation. *Cell Signal* **2006**, 18, 9-20.
58. Werman, A.; Hollenberg, A.; Solanes, G.; Bjorbaek, C.; Vidal-Puig, A. J.; Flier, J. S. Ligand-independent activation domain in the N terminus of peroxisome proliferator-activated receptor gamma (PPARgamma). Differential activity of PPARgamma1 and -2 isoforms and influence of insulin. *J Biol Chem* **1997**, 272, 20230-5.
59. Auwerx, J. PPARgamma, the ultimate thrifty gene. *Diabetologia* **1999**, 42, 1033-49.
60. Shao, D.; Rangwala, S. M.; Bailey, S. T.; Krakow, S. L.; Reginato, M. J.; Lazar, M. A. Interdomain communication regulating ligand binding by PPAR-gamma. *Nature* **1998**, 396, 377-80.
61. Hu, E.; Kim, J. B.; Sarraf, P.; Spiegelman, B. M. Inhibition of adipogenesis through MAP kinase-mediated phosphorylation of PPARgamma. *Science* **1996**, 274, 2100-3.
62. Nolte, R. T.; Wisely, G. B.; Westin, S.; Cobb, J. E.; Lambert, M. H.; Kurokawa, R.; Rosenfeld, M. G.; Willson, T. M.; Glass, C. K.; Milburn, M. V. Ligand binding and co-activator assembly of the peroxisome proliferator-activated receptor-gamma. *Nature* **1998**, 395, 137-43.



63. Gampe, R. T., Jr.; Montana, V. G.; Lambert, M. H.; Miller, A. B.; Bledsoe, R. K.; Milburn, M. V.; Kliewer, S. A.; Willson, T. M.; Xu, H. E. Asymmetry in the PPARgamma/RXRalpha crystal structure reveals the molecular basis of heterodimerization among nuclear receptors. *Mol Cell* **2000**, 5, 545-55.
64. Xu, H. E.; Lambert, M. H.; Montana, V. G.; Plunket, K. D.; Moore, L. B.; Collins, J. L.; Oplinger, J. A.; Kliewer, S. A.; Gampe, R. T., Jr.; McKee, D. D.; Moore, J. T.; Willson, T. M. Structural determinants of ligand binding selectivity between the peroxisome proliferator-activated receptors. *Proc Natl Acad Sci U S A* **2001**, 98, 13919-24.
65. Berger, J.; Moller, D. E. The mechanisms of action of PPARs. *Annu Rev Med* **2002**, 53, 409-35.
66. Nagy, L.; Schwabe, J. W. Mechanism of the nuclear receptor molecular switch. *Trends Biochem Sci* **2004**, 29, 317-24.
67. Glass, C. K.; Rosenfeld, M. G. The coregulator exchange in transcriptional functions of nuclear receptors. *Genes Dev* **2000**, 14, 121-41.
68. Hebbar, P. B.; Archer, T. K. Chromatin remodeling by nuclear receptors. *Chromosoma* **2003**, 111, 495-504.
69. Renaud, J. P.; Rochel, N.; Ruff, M.; Vivat, V.; Chambon, P.; Gronemeyer, H.; Moras, D. Crystal structure of the RAR-gamma ligand-binding domain bound to all-trans retinoic acid. *Nature* **1995**, 378, 681-9.
70. Willson, T. M.; Brown, P. J.; Sternbach, D. D.; Henke, B. R. The PPARs: from orphan receptors to drug discovery. *J Med Chem* **2000**, 43, 527-50.

71. Imai, T.; Takakuwa, R.; Marchand, S.; Dentz, E.; Bornert, J. M.; Messaddeq, N.; Wendling, O.; Mark, M.; Desvergne, B.; Wahli, W.; Chambon, P.; Metzger, D. Peroxisome proliferator-activated receptor gamma is required in mature white and brown adipocytes for their survival in the mouse. *Proc Natl Acad Sci U S A* **2004**, 101, 4543-7.
72. Kubota, N.; Terauchi, Y.; Miki, H.; Tamemoto, H.; Yamauchi, T.; Komeda, K.; Satoh, S.; Nakano, R.; Ishii, C.; Sugiyama, T.; Eto, K.; Tsubamoto, Y.; Okuno, A.; Murakami, K.; Sekihara, H.; Hasegawa, G.; Naito, M.; Toyoshima, Y.; Tanaka, S.; Shiota, K.; Kitamura, T.; Fujita, T.; Ezaki, O.; Aizawa, S.; Kadowaki, T.; et al. PPAR gamma mediates high-fat diet-induced adipocyte hypertrophy and insulin resistance. *Mol Cell* **1999**, 4, 597-609.
73. Bays, H.; Mandarino, L.; DeFronzo, R. A. Role of the adipocyte, free fatty acids, and ectopic fat in pathogenesis of type 2 diabetes mellitus: peroxisomal proliferator-activated receptor agonists provide a rational therapeutic approach. *J Clin Endocrinol Metab* **2004**, 89, 463-78.
74. Oakes, N. D.; Thalen, P. G.; Jacinto, S. M.; Ljung, B. Thiazolidinediones increase plasma-adipose tissue FFA exchange capacity and enhance insulin-mediated control of systemic FFA availability. *Diabetes* **2001**, 50, 1158-65.
75. Smith, M. T. Mechanisms of troglitazone hepatotoxicity. *Chem Res Toxicol* **2003**, 16, 679-87.

76. Chiarelli, F.; Di Marzio, D. Peroxisome proliferator-activated receptor-gamma agonists and diabetes: current evidence and future perspectives. *Vasc Health Risk Manag* **2008**, 4, 297-304.
77. Diamant, M.; Heine, R. J. Thiazolidinediones in type 2 diabetes mellitus: current clinical evidence. *Drugs* **2003**, 63, 1373-405.
78. Lebovitz, H. E.; Dole, J. F.; Patwardhan, R.; Rappaport, E. B.; Freed, M. I. Rosiglitazone monotherapy is effective in patients with type 2 diabetes. *J Clin Endocrinol Metab* **2001**, 86, 280-8.
79. Miyazaki, Y.; Mahankali, A.; Matsuda, M.; Glass, L.; Mahankali, S.; Ferrannini, E.; Cusi, K.; Mandarino, L. J.; DeFronzo, R. A. Improved glycemic control and enhanced insulin sensitivity in type 2 diabetic subjects treated with pioglitazone. *Diabetes Care* **2001**, 24, 710-9.
80. Roussel, A.; Fontecilla-Camps, J. C.; Cambillau, C. CRYStallize: a crystallographic symmetry display and handling subpackage in TOM/FRODO. *J Mol Graph* **1990**, 8, 86-8, 91.
81. Emsley, P.; Cowtan, K. Coot: model-building tools for molecular graphics. *Acta Crystallogr D Biol Crystallogr* **2004**, 60, 2126-32.
82. Waku, T.; Shiraki, T.; Oyama, T.; Morikawa, K. Atomic structure of mutant PPARgamma LBD complexed with 15d-PGJ2: novel modulation mechanism of PPARgamma/RXRalpha function by covalently bound ligands. *FEBS Lett* **2009**, 583, 320-4.

83. Cozzini, P.; Fornabaio, M.; Marabotti, A.; Abraham, D. J.; Kellogg, G. E.; Mozzarelli, A. Simple, intuitive calculations of free energy of binding for protein-ligand complexes. 1. Models without explicit constrained water. *J Med Chem* **2002**, 45, 2469-83.
84. Hansch, C. The interaction of ligands with enzymes. A starting point in drug design. *Farmaco [Sci]* **1979**, 34, 729-42.
85. Kellogg, G. E.; Abraham, D. J. Hydrophobicity: is LogPo/w more than the sum of its parts? *European Journal of Medicinal Chemistry* **2000**, 35, 651-661.
86. Fornabaio, M.; Spyraakis, F.; Mozzarelli, A.; Cozzini, P.; Abraham, D. J.; Kellogg, G. E. Simple, intuitive calculations of free energy of binding for protein-ligand complexes. 3. The free energy contribution of structural water molecules in HIV-1 protease complexes. *J Med Chem* **2004**, 47, 4507-16.
87. Kellogg, G. E.; Fornabaio, M.; Chen, D. L.; Abraham, D. J.; Spyraakis, F.; Cozzini, P.; Mozzarelli, A. Tools for building a comprehensive modeling system for virtual screening under real biological conditions: The Computational Titration algorithm. *J Mol Graph Model* **2006**, 24, 434-9.
88. Kuo, C. F.; McRee, D. E.; Cunningham, R. P.; Tainer, J. A. Purification, crystallization and space group determination of DNA repair enzyme exonuclease III from *E. coli*. *J Mol Biol* **1993**, 229, 239-42.
89. Bruning, J. B.; Chalmers, M. J.; Prasad, S.; Busby, S. A.; Kamenecka, T. M.; He, Y.; Nettles, K. W.; Griffin, P. R. Partial agonists activate PPARgamma using a helix 12 independent mechanism. *Structure* **2007**, 15, 1258-71.

90. Ambrosio, A. L.; Dias, S. M.; Polikarpov, I.; Zurier, R. B.; Burstein, S. H.; Garratt, R. C. Ajulemic acid, a synthetic nonpsychoactive cannabinoid acid, bound to the ligand binding domain of the human peroxisome proliferator-activated receptor gamma. *J Biol Chem* **2007**, 282, 18625-33.
91. Klebe, G. Recent developments in structure-based drug design. *J Mol Med* **2000**, 78, 269-81.

## VITA

Ashwini Goswami was born on November 12, 1977 in Narwana, Haryana state of India and is an Indian citizen. He obtained a Bachelor's degree in Pharmaceutical sciences (B. Pharmacy) in 2001 from Maharshi Dayanand University Rohtak, India. Ashwini joined the M.S. program in the Department of Medicinal Chemistry, School of Pharmacy at Virginia Commonwealth University in fall 2005 and subsequently joined Dr. Martin Safo's lab in spring 2006 to begin work on development of PPAR- $\gamma$  receptor agonists as therapeutic agents for diabetes.